

**INVESTIGATING THE ANTI-  
INFLAMMATORY MECHANISM OF  
THE ADIPONECTIN RECEPTOR  
AGONIST, ALY688, IN IRON  
OVERLOAD-INDUCED  
MACROPHAGE ACTIVATION**

**BOJUN ZHANG**

**A THESIS SUBMITTED TO THE FACULTY OF GRADUATE  
STUDIES IN PARTIAL FULFILLMENT OF THE REQUIREMENTS  
FOR THE DEGREE OF MASTER OF SCIENCE**

**GRADUATE PROGRAM IN BIOLOGY**

**YORK UNIVERSITY, TORONTO, ONTARIO**

**July 2025**

**© Bojun Zhang, 2025**

## ABSTRACT

Chronic inflammation, driven by factors such as iron overload, contributes to metabolic, cardiovascular, and degenerative diseases. Excess iron promotes pro-inflammatory cytokines release and increased production of reactive oxygen species (ROS) in macrophages via transcription factors, such as IRF and NF- $\kappa$ B. This study investigated whether ALY688, an adiponectin receptor agonist, mitigate iron-induced inflammation. Using ferrous sulfate ( $\text{FeSO}_4$ ) treated RAW 264.7 macrophages, I found that ALY688 markedly reduced the activation of both NF- $\kappa$ B and IRF pathways, suppressed ROS levels, and reversed the expression of inflammatory and antioxidant genes. Iron overload significantly upregulated pro-inflammatory cytokines (IL-1 $\beta$ , TNF- $\alpha$ , IL-6) and oxidative stress-related genes (NOX2), while downregulating anti-inflammatory mediators such as IL-10. Together, these findings support a regulatory role of ALY688 in attenuating iron-induced oxidative stress and inflammation in macrophages, suggesting that ALY688 may serve as a promising therapeutic candidate for iron overload-associated inflammatory disorders.

## **ACKNOWLEDGEMENTS**

I would like to express my deepest gratitude to my supervisor, Dr. Gary Sweeney, and our lab manager, Dr. Hyekyoung (Cindy) Sung, for offering me the opportunity to join the lab two years ago. Their trust and support have allowed me to embark on this research journey and grow as an independent scientist. I am truly thankful for their continuous guidance, patience, and encouragement throughout the course of my MSc studies.

I also wish to thank the members of our lab for their assistance and valuable feedback. Special thanks to Eddie Tam, Sungi Cho, Wing Yan Chung, and Yue Qu for providing thoughtful advice and technical support during key stages of the project.

I would like to extend my appreciation to Dr. Robert Tsushima for his feedback regarding my research progress and presiding over my defense, and to my examining committee members, Dr. Yuqing Feng and Dr. Anthony Scimè, for taking the time to evaluate my thesis and provide constructive feedback.

Finally, I am profoundly grateful to my family for their unwavering love and support. I especially want to thank my husband, Yuchen Yang, who made the tremendous personal sacrifice of leaving a job he loved in order to accompany and support me during my studies in Canada. Their support and encouragement gave me the strength to face every challenge along the way.

Last but not least, I would like to thank myself – for pushing through the most challenging moments, especially during the time when I was unwell. I am proud of the resilience and determination that carried me through to the end of this journey.

## **ABBREVIATIONS**

AdipoR\_\_adiponectin receptor

CVD\_\_cardiovascular disease

cGAS-STING\_\_ cyclic GMP-AMP synthase- Stimulator of interferon genes

COX\_\_cyclooxygenase

HFE\_\_high iron Fe

NADPH\_\_nicotinamide adenine dinucleotide phosphate (reduced form)

NOX\_\_NADPH oxidase

IFN\_\_interferon regulatory factor

IL-1 $\beta$ \_\_interleukin-1 beta

ISG\_\_interferon-stimulated genes

MRI\_\_magnetic resonance imaging

NALD \_\_non-alcoholic fatty liver disease

PBS \_\_phosphate-buffered saline

RIG-1\_\_retinoic acid- inducible gene I

T2D \_\_type 2 diabetes

TLR\_\_toll like receptor

TNF- $\alpha$ \_\_tumor necrosis factor alpha

## Table of Contents

ABSTRACT.....	ii
ACKNOWLEDGEMENTS.....	iii
ABBREVIATION.....	v
1 CHAPTER 1: LITERATURE REVIEW.....	1
1.1 Iron metabolism.....	2
1.2 Pathological and clinical implications of iron overload.....	7
1.3 Iron overload and oxidative stress.....	10
1.4 Iron overload-induced inflammation: from innate immunity to chronic diseases.....	12
1.5 Classical inflammatory signaling pathways.....	15
1.6 The role of macrophages.....	19
1.7 Adipose tissue and inflammation.....	22
1.8 Adiponectin: structure and function.....	24
1.9 ALY688: a novel adiponectin receptor agonist.....	25
2 CHAPTER 2: <i>ALY688 attenuates iron overload-induced inflammation in RAW 264.7 macrophages by reducing oxidative stress</i> .....	29
2.1 Hypothesis.....	30
2.2 Study aims and significance.....	31
2.3 Experimental models.....	32
2.4 Methods.....	33
2.5 Results.....	41

2.6 Discussion.....	51
2.7 Conclusion.....	56
3 CHAPTER 3: CONCLUSIONS.....	57
3.1 Thesis Summary.....	58
3.2 Study Limitations.....	59
3.3 Future Works.....	60
REFERENCES.....	62

## **Chapter 1**

### **LITERATURE REVIEW**

## 1.1 Iron metabolism

Iron is an essential mineral micronutrient, playing a pivotal role in various physiological processes within almost all organisms' bodies, such as facilitating oxygen transport through its role in hemoglobin, participating in cellular respiration, and supporting DNA synthesis [1]. As a transitional metal, iron can donate and accept electrons alternately in oxidation-reduction reactions, and thereby offers advantages for fundamental biological processes [2]. Under normal physiological conditions, iron exists in multiple oxidative states and continually transitions between them [3]. Ferric iron ( $\text{Fe}^{3+}$ ) is the predominant form in the circulation, where it is bound to transferrin for safe transport, while ferrous iron ( $\text{Fe}^{2+}$ ) is mainly found intracellularly, where it participates in metabolic and enzymatic processes [4]. Ferric iron is the relatively more stable form with low solubility in aqueous environments [3]. To address this limitation and maintain adequate bioavailability, ferric iron is typically bound to carrier proteins such as transferrin [3, 5]. This binding not only enhances its solubility but also allows iron to circulate in a redox-inactive and safe form [6]. In contrast, ferrous iron ( $\text{Fe}^{2+}$ ) is more water-soluble and highly reactive, contributing to its cytotoxic potential [3, 6].

Cellular iron homeostasis is precisely regulated by a network of transport, storage, utilization, and export mechanisms [7]. As shown in figure 1, the cellular uptake of iron complexed with transferrin occurs via

endocytosis mediated by transferrin receptor 1 (TfR1) [8]. Subsequently, iron in the endosomal lumen is reduced from its ferric to ferrous form by the action of six-transmembrane epithelial antigen of prostate 3 (STEAP3). The resulting ferrous iron ( $\text{Fe}^{2+}$ ) is then transported into the cytoplasm by divalent metal transporter 1 (DMT1), contributing to the labile iron pool (LIP) [8]. This pool represents metabolically available iron and serves as the source for mitochondrial iron utilization, including heme synthesis and iron-sulfur cluster (ISC) assembly, both essential for enzymatic reactions and electron transport [8, 9]. Excess intracellular iron is safely stored in ferritin, a multi-subunit protein complex capable of sequestering thousands of iron atoms in a redox-inert form [10]. In response to sufficient intracellular iron levels, ferroportin (FPN1), the only known iron exporter in mammals, can facilitate iron release from cells [11].

While genetic regulatory controls occur at various stages, post-transcriptional control facilitated by the iron-responsive element/ iron regulatory protein (IRE/IRP) system is recognized as pivotal and indispensable [12, 13]. The IRE/IRP system controls various mRNAs encoding proteins for iron metabolism, for example, the mRNAs encoding transferrin receptor 1 (TFRC-TFR1), ferritin H (FTH1), and ferritin L (FTHL) [14, 15]. The regulation of cellular iron metabolism involves the binding of IRP1 or IRP2 to specific mRNA motifs known as IREs in the 5' untranslated region (UTR), blocking translation, such as FTH1 and FTL2 [16]. Also, IRP

binding to IREs in the 3'UTR of TFR1 mRNA can protect it from degradation [12]. The IRE-binding capacity of IRP1 and IRP2 is elevated in iron-insufficient cells and diminished in cells with adequate iron levels; therefore, an increased intracellular iron level can bring an elevated ferritin level, while a decreased iron level will result in a raised transferrin level, meaning iron is brought to the cell from the circulatory system [12]. When the iron is sufficient, an ISC forms in IRP1, preventing it from binding to IREs [12]. During the period of iron deficiency, IRP1 undergoes conformational changes and eventually binds to IRE2. IRP2 lacks an ISC, and its regulation is controlled by iron through proteasomal degradation [12]. Both IRP1 and IRP2's IRE-binding abilities ensure the regulation of expressions of genes targeted by IRPs and maintain intracellular iron homeostasis [12].

Systemic regulation of iron homeostasis is centrally regulated by hepcidin, a key peptide hormone synthesized in the liver. Hepcidin controls iron efflux by binding to ferroportin, triggering its ubiquitination, internalization, and lysosomal degradation [17]. This process limits the release of intracellular iron to the bloodstream [18]. Thus, when systemic iron level is elevated, hepcidin concentration increases, leading to the internalization and degradation of ferroportin [18]. As a result, intracellular iron export is suppressed, reducing its entry into the circulation [18]. However, when the blood iron level is low, hepcidin concentration is reduced, allowing ferroportin to remain on the cell surface, therefore,

facilitating iron release into the blood stream [18]. Hepcidin expression is regulated not only by systemic iron levels but also by erythropoietic activity and hypoxia, creating an integrated feedback system that maintains overall iron homeostasis in the body [19]. These regulatory mechanisms work together to ensure precise control of iron metabolism, balancing its essential biological functions with the potential risk of toxicity.

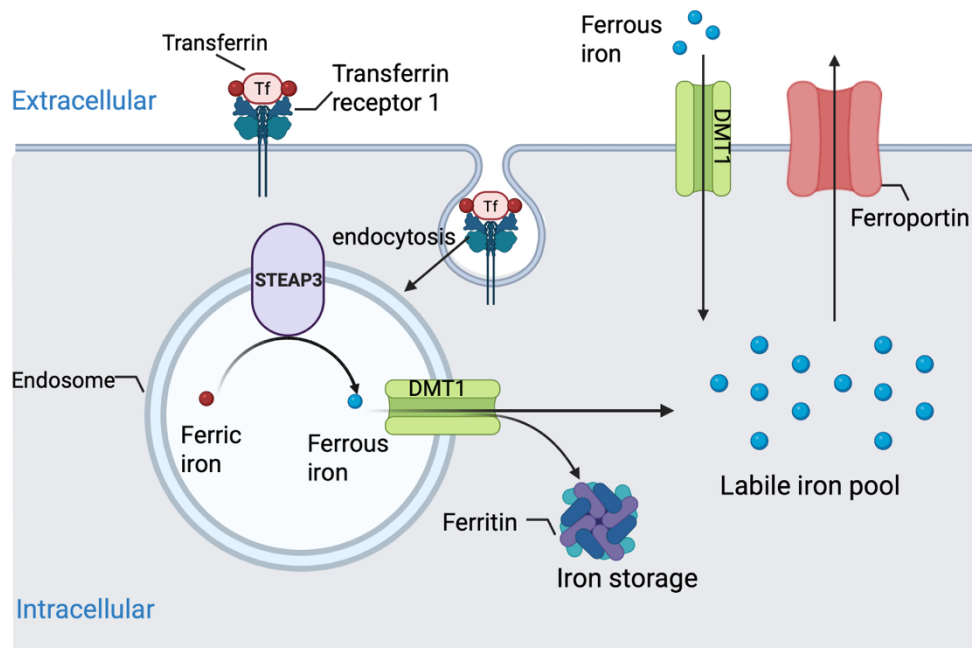


**Figure 1. Cellular iron uptake and intracellular iron homeostasis mediated by transferrin receptor1 and ferroportin.**

Circulating transferrin (Tf) delivers ferric iron to cells via binding to TFR1 on the cell surface. The Tf-Fe<sup>3+</sup>-TFR1 complex is internalized through endocytosis, forming an endosome. Within the acidic endosomal environment, ferric iron is reduced to ferrous iron by STEAP3. The ferrous iron is then transported into the cytosol via a divalent metal transporter named DMT1, contributing to the labile iron pool. Excess intracellular iron can be stored safely in ferritin or exported out of the cell via ferroportin. This pathway ensures precise regulation of iron availability, preventing toxicity while maintaining essential cellular functions. Created with BioRender.com. Adapted from Tam, 2023 [20].

## **1.2 Iron overload in pathological and clinical contexts**

Both excessive and insufficient iron levels can have harmful effects on cellular function and be detrimental to the body [21]. Iron deficiency is related to a number of health issues, such as impaired oxygen transport, cognitive impairment, and increased risk of heart failure [21]. At the cellular level, iron deficiency can lead to cellular growth arrest and, ultimately, cell death [22, 23]. However, excessive iron levels can be detrimental to the cells and harmful to the body [24]. There is no naturally efficient physiological pathway for iron excretion other than blood loss, making the body particularly vulnerable to iron-induced toxicity when iron levels become excessive [3]. Therefore, to minimize the cytotoxic potential of iron while preserving its biological functions in numerous proteins, both systemic and cellular iron levels must be strictly regulated.

In normal physiological conditions, total body iron content ranges from approximately three to five grams. Clinically, iron status is assessed by using serum biomarkers [25]. The normal range of serum ferritin level is 30-300 ng/ml in males and 10-200 ng/ml in females [26]. Serum transferrin saturation (TSAT) is calculated as the ratio of serum iron concentration to the total iron-binding capacity, typically ranging from 20% to 40% [27]. TSAT below 20% indicates iron deficiency, while values above 45% suggest iron overload [27]. Serum iron concentrations are generally

between 10 and 30  $\mu\text{M}$ , and levels exceeding 89.5  $\mu\text{M}$  are associated with an increased risk of toxicity [28].

The diagnosis of iron overload in clinical settings primarily relies on blood-based assays, including measurements of serum ferritin, TSAT, and serum iron levels. Although these are indirect indicators, they are cost-effective, non-invasive, and suitable for routine screening. In more definitive cases, liver biopsy is still considered the gold standard for evaluating iron accumulation, though it is invasive and less commonly performed [29]. Non-invasive imaging techniques such as MRI T2 are increasingly used to evaluate tissue iron deposition, especially in the liver and heart [30, 31]. Additional biomarkers, such as hepcidin and soluble transferrin receptor (sTfR) can provide further information on iron metabolism status [32, 33].

When iron accumulates in the body and exceeds the normal capacity, it can lead to iron overload, or hemochromatosis, a pathological condition contributing to various chronic disorders, including cardiovascular disease, metabolic syndrome, and neurodegenerative disorders [34, 35]. Hemochromatosis is broadly classified into primary and secondary forms, with primary hemochromatosis accounting for most cases, prevalently resulting from genetic mutations affecting iron absorption or regulation [36]. Five genetic types have been identified: mutations in the HFE gene for type 1, hemojuvelin for type 2A, hepcidin for type 2B, transferrin receptor 2 for type 3, and ferroportin for type 4 [37]. Among these, HFE-associated

hemochromatosis accounting for the most prevalent, especially in Northern European populations [36]. Most of these genetic disorders result in decreased or absent hepcidin expression, leading to unregulated intestinal iron absorption and progressively accumulated iron in multiple organs, such as the heart, liver and pancreas [38].

Secondary iron overload occurs in the context of external iron loading, most frequently due to repeated blood transfusions in conditions like  $\beta$ -thalassemia and sickle cell anemia, or due to excessive dietary iron intake [39]. Regardless of the cause, iron overload is associated with numerous complications, including hepatic fibrosis and cirrhosis, cardiomyopathy, diabetes mellitus, arthritis, and an increased risk of hepatocellular carcinoma. Treatment strategies depend on the underlying cause: therapeutic phlebotomy is the first-line approach for hereditary hemochromatosis, also the cheapest and most effective method, whereas iron chelation therapy is used in transfusion-related cases to facilitate iron excretion through the urine or feces [40, 41].

On the cellular level, excess iron can be detrimental as well. When present in excess, ferrous iron participates in the Fenton reaction, catalyzing the formation of reactive oxygen species (ROS), inducing oxidative stress and finally leading to cell death and tissue injury with the heart, liver, pancreas, and central nervous system being particularly vulnerable [40].

### 1.3 Iron overload and oxidative stress

ROS are highly reactive chemical molecules derived from molecular oxygen, including superoxide anions ( $O_2^-$ ), hydroxyl radicals ( $\bullet OH$ ), and hydrogen peroxide ( $H_2O_2$ ) [42]. ROS are generated as byproducts of essential biological processes, including cellular respiration and oxidative phosphorylation. These ROS are mainly produced in cellular organelles such as endoplasmic reticulum, mitochondria, and peroxisomes [42]. To maintain redox homeostasis, cells are equipped with a range of antioxidant systems, including enzymatic and non-enzymatic defenses. Key enzymes involved in the antioxidant defense systems include superoxide dismutase (SOD), glutathione peroxidase (GPx), and catalase [43]. Among them, SOD plays a crucial role in defense against oxidative stress by catalyzing the dismutation of superoxide radicals into hydrogen peroxide and oxygen [43]. GPx families use glutathione as a reducing agent to convert hydrogen peroxide and other organic hydroperoxides into water and alcohols, thereby protecting various cellular compartments from oxidative damage [44]. Catalase can neutralize hydrogen peroxide by converting it into harmless water and oxygen [45]. In Santanam and colleague's study, the overexpression of catalase can trigger protective effects in mitigating oxidative injury in vascular cells [46]. Non-enzymatic antioxidants primarily consist of vitamins, minerals, and some metabolites, for example vitamin C, zinc, and uric acid [43]. Uric acid has been shown to protect against

peroxynitrite-induced damage by inhibiting protein nitrosylation, lipid and protein peroxidation, and the deactivation of tetrahydrobiopterin, thereby acting as a free radical scavenger and chelator of transition metal iron [47]. Although often associated with oxidative damage, low concentrations of ROS under normal physiological conditions can act as signaling molecules involved in cell survival, differentiation, and proliferation [48]. However, when the balance between ROS production and antioxidant capacity is disrupted—due to increased ROS generation or impaired detoxification mechanisms—oxidative stress occurs. Persistent oxidative stress contributes to the oxidation of nucleic acids, proteins, and lipids, leading to cellular damage, dysfunction, and death. Numerous studies have reported that oxidative stress is related to the pathogenesis of various health disorders, including cardiovascular disease, neurodegeneration, insulin resistance, and cancer [49-52].

Iron overload is a key driver of oxidative stress due to iron's redox-active nature and its ability to catalyze ROS formation through Haber-Weiss and Fenton reaction [53] [54]. In Haber-Weiss reaction, superoxide reduces ferric iron to ferrous iron, producing molecular oxygen [55]. The next step is the Fenton reaction, where the ferrous iron reacts with hydrogen peroxide ( $H_2O_2$ ) to generate hydroxyl radicals ( $\bullet OH$ ), among the most reactive and damaging ROS [54]. Under normal conditions, iron is safely stored within ferritin or bound to hemoglobin and transferrin, thereby limiting its pro-

oxidant activity [10]. However, in conditions of iron overload—whether primary, due to genetic disorders such as hereditary hemochromatosis, or secondary, as seen in chronic transfusion therapy—excess free iron accumulates in tissues [10]. The elevated cellular iron level promotes uncontrolled ROS generation, overwhelming cellular antioxidant defenses and inducing oxidative damage to biomolecules [8]. Moreover, iron-induced lipid peroxidation contributes to cell death via ferroptosis, a form of iron-dependent non-apoptotic necrosis characterized by the accumulation of lipid hydroperoxides [56]. The persistent presence of ROS under iron overload conditions is linked to the progression of tissue fibrosis, organ dysfunction, and chronic metabolic diseases.

#### **1.4 Iron overload- induced inflammation: From innate immunity to chronic diseases**

The immune system is essential for maintaining physiological homeostasis, not only by defending against pathogens but also by regulating inflammation, promoting tissue regeneration, and preventing autoimmunity. The immune system is conventionally divided into two independent types: innate and adaptive immunity. The Innate immunity provides the first line of defense in the body and is characterized by a rapid and non-specific response to invading pathogens or tissue damage. Its protective functions are mediated by innate immune cells, for example,

macrophages, dendritic cells, and neutrophils [57]. These innate immune cells can detect the presence of danger through pattern recognition receptors (PRRs) expressed on their surface [57]. PRRs recognize conserved molecular structures termed pathogen-associated molecular patterns (PAMPs) and damage-associated molecular patterns (DAMPs), upon which they become activated and initiated intracellular signaling cascades [57]. As a result, these pathways leading to the production of chemokines, pro-inflammatory cytokines, and type I interferons, ultimately initiate the inflammatory response [58]. In contrast, adaptive immunity provides a slower but highly specific response, mediated by antigen-presenting cells, T cells, and B cells. Within this framework, inflammation is a hallmark response of innate immunity, initiated immediately upon recognition of threats, and is essential for containing infection and initiating tissue repair [59].

Inflammation is a localized and complex physiological process that arises in response to infections, physical injuries, or other harmful stimuli [59]. Its primary function is to eliminate the initial cause of cellular damage, clear out necrotic cells and tissues, and initiate repair mechanisms [59]. Hallmarks of inflammation include swelling, redness, pain, increased temperature, and function impairment, which result from increased blood flow, vascular permeability, and leukocyte infiltration [60-62]. In the acute phase, inflammation is usually self-limiting and resolves once the stimulus

is eliminated [63]. However, when the inflammatory trigger persists or regulatory mechanisms fail, chronic inflammation can develop, leading to prolonged immune activation, tissue remodeling, and pathological consequences. Chronic inflammation plays a central role in the development of many non-communicable diseases, including cardiovascular disorders, metabolic syndromes, and neurodegeneration [64, 65].

Iron overload has been increasingly recognized as a driver of chronic inflammation both directly and indirectly, particularly through its ability to catalyze the production of ROS via the Fenton reaction. As previously discussed in Section 1.3, ROS are key mediators of oxidative stress. By activating redox-sensitive transcription factors such as NF- $\kappa$ B and AP-1, ROS contribute to the upregulation of pro-inflammatory cytokines including IL-1 $\beta$ , IL-6, and TNF- $\alpha$  [66, 67]. Excess iron preferentially accumulates in macrophages, which respond by adopting a pro-inflammatory phenotype [68]. This skewed macrophage polarization contributes to low-grade, chronic inflammation observed in conditions such as atherosclerosis, type 2 diabetes, and  $\beta$ -thalassemia [68]. Additionally, iron participates in the oxidation of low-density lipoproteins (LDL), further fueling vascular inflammation and plaque formation [69]. Hence, iron overload is not merely a byproduct but an active amplifier of chronic

inflammatory responses, posing long-term risks to tissue integrity and systemic health.

### **1.5 Classical inflammatory signaling pathways**

Among the molecular mechanisms that related to inflammatory responses, several conserved signaling pathways play pivotal roles in transmitting extracellular danger signals to transcriptional responses [70]. Notably, the nuclear factor kappa-light-chain-enhancer of activated B cells (NF- $\kappa$ B) and interferon regulatory factor (IRF) pathways are the two key signaling axes that regulate the production of pro-inflammatory cytokines and interferons [70]. Understanding these pathways is essential for elucidating how cells detect and respond to inflammatory stimuli, particularly in the context of stressors such as iron overload or PAMPs.

The canonical NF- $\kappa$ B pathway plays a crucial role in regulating genes involved in immune responses, inflammation, and cell survival. In resting cells, NF- $\kappa$ B dimers are sequestered in the cytoplasm by inhibitors of  $\kappa$ B (I $\kappa$ B) proteins [70]. Upon activation by stimuli such as LPS, TNF- $\alpha$ , or oxidative stress, the I $\kappa$ B kinase (IKK) complex is activated, leading to phosphorylation and subsequent proteasomal degradation of I $\kappa$ B [70]. This allows NF- $\kappa$ B dimers to translocate from the cytoplasm into the nucleus and then initiate the transcription of target genes, including IL-1 $\beta$ , IL-6, TNF- $\alpha$ , and COX-2 [71-73]. Persistent activation of NF- $\kappa$ B has been implicated in

the pathogenesis of various inflammatory conditions, including atherosclerosis, rheumatoid arthritis, and cancer [74-76].

The IRF family of transcription factors is primarily involved in the regulation of type I interferon responses and antiviral immunity. Among them, IRF3 and IRF7 are critical for the induction of interferon- $\alpha$  and interferon- $\beta$  following recognition of viral nucleic acids by pattern recognition receptors such as TLRs or cytosolic sensors like RIG-I and cGAS-STING [77]. TLRs are membrane-bound receptors that detect extracellular or endosomal pathogen-associated molecules, while RIG-I and cGAS-STING are cytosolic sensors that recognize viral RNA or DNA within the cells [78]. Certain TLRs exhibit lineage-specific response patterns. For example, although both monocytes and macrophages express comparable levels of TLR4, only macrophages induce the expression of ISGs following TLR4 activation [79]. Upon activation, IRFs undergo phosphorylation, dimerization, and nuclear translocation, where they drive the expression of interferons and ISGs[80]. Beyond their role in antiviral defense, IRFs have also been implicated in sterile inflammation, autoimmune diseases, and modulating macrophage polarization[80]. IRF-mediated pathways can interact with NF- $\kappa$ B signaling, contributing to the complexity and specificity of inflammatory responses[81].

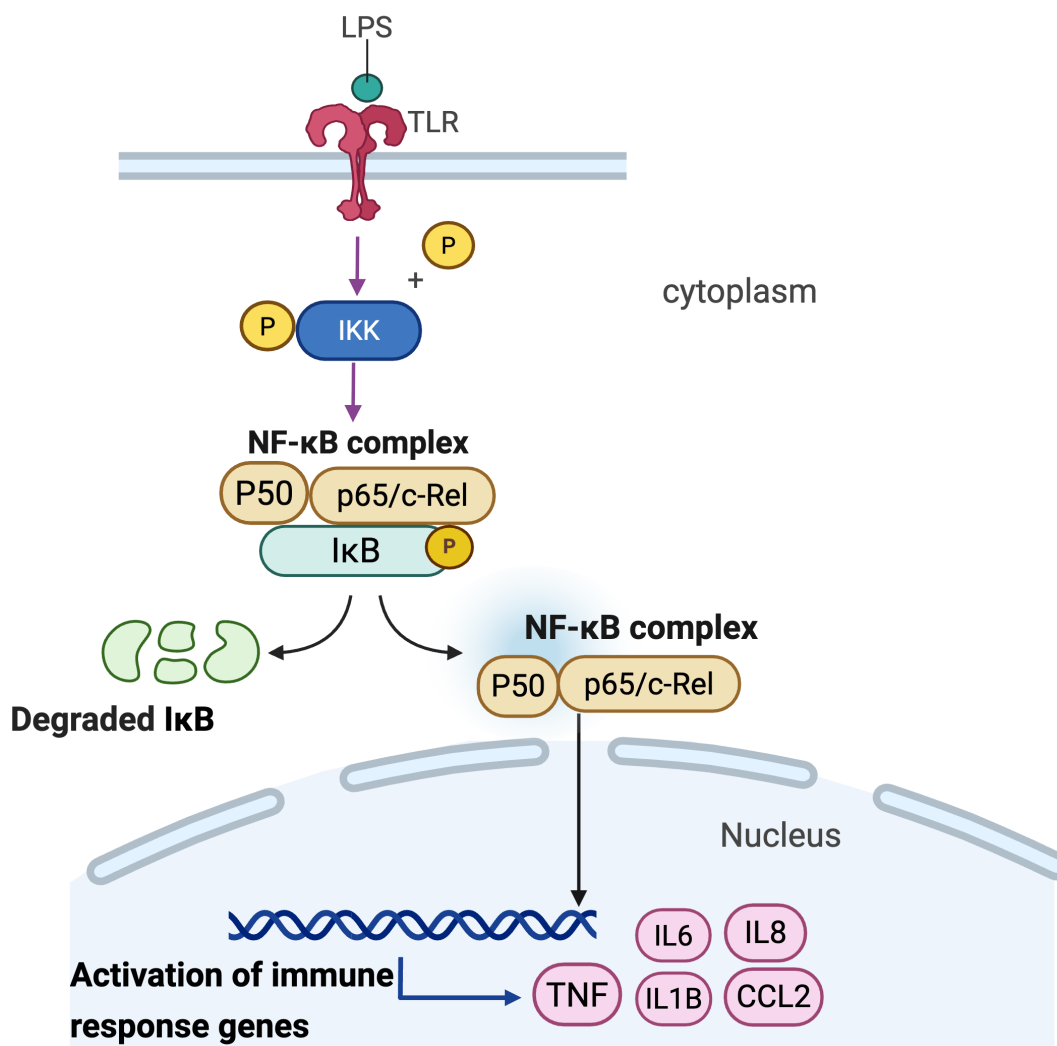


**Figure 2. NF-κB signaling pathway**

Upon recognition of LPS by toll-like receptors TLRs, the IKK complex becomes activated and phosphorylates the inhibitory IκB protein. This leads to the ubiquitin-mediated degradation of IκB, allowing the NF-κB heterodimer (typically p50/p65 or p50/c-Rel) to translocate into the nucleus. Once in the nucleus, NF-κB binds to κB motifs on DNA and activates the transcription of immune response genes. Created with BioRender.com. Adapted from Liu et al., 2017 [70].

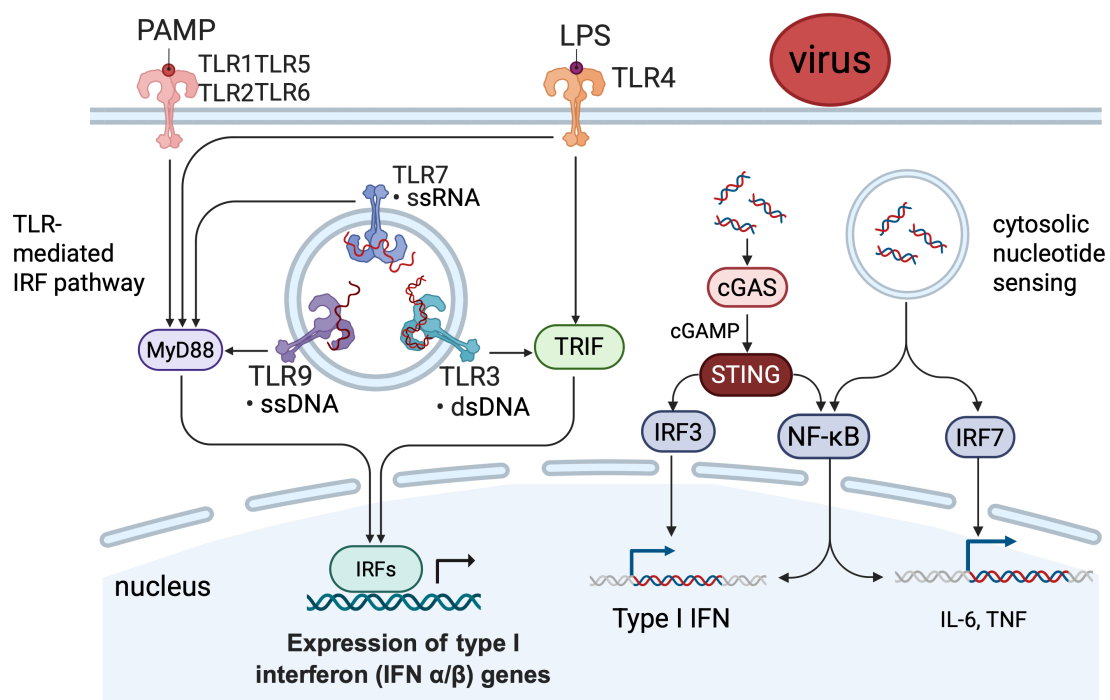


**Figure 3. Schematic overview of the IRF pathways leading to type I interferon production.** Both TLRs and cytosolic DNA sensors (eg. cGAS) activate IRF3/7 through distinct adaptor proteins (MyD88, TRIF, STING), resulting in type I interferon gene expression. These pathways also engage NFκB to promote proinflammatory cytokine production. Created with BioRender.com. Adapted from Lukhele et al., 2019 [82].

## 1.6 The role of macrophages

Macrophages are important immune cells of the innate immune system, acting as both sentinels and effectors in the host's response to invasive infection and tissue damage [83]. They perform diverse functions including phagocytosis of pathogens and debris, antigen presentation, and secretion of inflammatory mediators [83]. Once macrophages encounter danger signals such as PAMPs or DAMPs, they can initiate intracellular signaling cascades that result in the production of chemokines, cytokines, and interferons [84, 85]. The release of these mediators leads to the recruitment and activation of other immune cells, ultimately shaping both the local inflammatory environment and the downstream adaptive immune response [85]. In addition to defending against pathogens, macrophages also play crucial roles in maintaining tissue homeostasis, supporting repair, and resolving inflammation once the insult has been cleared [86, 87].

For decades, macrophages were classified into M1, the pro-inflammatory, and M2, the anti-inflammatory subtypes based on in vitro stimuli and surface markers. However, growing research evidence suggests that the classical polarization model does not accurately reflect the true diversity of macrophage behavior in organisms [88]. Insights from single-cell RNA sequencing and lineage tracing have shown that macrophages display a broad spectrum of activation states shaped by their environment, rather than in discrete M1 or M2 states [88]. Notably,

commonly used markers like CCR2 and CD206 are not exclusive to M1 or M2 macrophages and are variably expressed depending on tissue context and cell origin [88, 89]. Furthermore, the traditional view that all macrophages arise from circulating monocytes has been revised [88]. It is now recognized that many tissue-resident macrophages originate from embryonic progenitors and possess self-renewing capacity, independent of monocyte replenishment [88, 90]. These insights have prompted a paradigm shift toward classifying macrophages based on transcriptional signatures, ontogeny, and microenvironmental cues, rather than oversimplified binary states [88].

Iron overload exerts profound effects on macrophage phenotype and function [91]. Under conditions of excess iron, macrophages exhibit enhanced oxidative stress as a result of elevated production of reactive oxygen species (ROS), primarily via the Fenton reaction [92]. This redox imbalance leads to the activation of pro-inflammatory signaling pathways such as NF- $\kappa$ B, resulting in increased secretion of cytokines including IL-1 $\beta$ , IL-6, and TNF- $\alpha$  [93]. Iron-loaded macrophages also display impaired phagocytic capacity and altered expression of iron-regulatory proteins, such as ferroportin and ferritin [94, 95]. These changes not only compromise the homeostatic functions of macrophages but also contribute to sustained low-grade inflammation observed in diseases such as atherosclerosis,  $\beta$ -thalassemia, and metabolic syndrome [96, 97]. While the

M1/M2 polarization framework has been widely used to describe macrophage functional states, recent studies suggest that it oversimplifies the complex and context-dependent heterogeneity of macrophages, particularly tissue-resident subsets [88, 98]. High-dimensional single-cell analyses have revealed transcriptionally distinct macrophage populations that cannot be adequately captured by the M1/M2 model [88]. Recent studies further suggest that iron overload may skew macrophage polarization toward a pro-inflammatory state, although this shift does not strictly correspond to the classical M1 phenotype, reflecting instead a complex reprogramming of immune-metabolic functions [68, 88, 99]

Macrophages are uniquely sensitive to fluctuations in iron availability due to their central role in iron metabolism. As professional phagocytes, they are responsible for the clearance of senescent red blood cells and the recycling of hemoglobin-derived iron, making them key regulators of systemic iron homeostasis. Compared to other cell types, macrophages express high levels of ferroportin for iron export and ferritin for iron storage [100]. Because of their constant exposure to iron, they are especially vulnerable to oxidative stress when iron homeostasis is disrupted [94, 101]. Even modest elevations in the macrophages' labile iron levels can initiate Fenton reaction, producing hydroxyl radicals that damage cellular components and activate inflammatory responses [102]. These characteristics make macrophages not only primary sensors of iron

imbalance but also active effectors in iron-overload–associated inflammation.

### **1.7 Adipose tissue and inflammation**

Adipose tissue, composed mainly of adipocytes and a supportive stromal vascular fraction, serves as a critical regulator of systemic energy balance [103]. During nutrient abundance, adipose tissue stores the body's excess energy in the form of triglycerides. Conversely, it mobilizes free fatty acids during fasting. Adipose tissue functions not only as a storage site for excess energy but also as a metabolically active endocrine organ that releases various hormones, collectively known as adipokines, including adiponectin, leptin, resistin, and visfatin [104]. Adipokines can influence appetite control, insulin sensitivity, lipid metabolism, and immune responses [105]. Adipose tissue is broadly classified into two different types: white adipose tissue (WAT) and brown adipose tissue (BAT) [106]. WAT mainly functions in energy storage, while BAT spends energy as heat via non-shivering thermogenesis [107]. Adipose tissue comprises not only adipocytes but also various other cell types, including immune cells, preadipocytes, endothelial cells, and fibroblasts, which collectively contribute to its immunometabolic functions [108, 109].

Under physiological conditions, adipose tissue contributes to immune homeostasis by producing anti-inflammatory adipokines such as

adiponectin, which enhances insulin sensitivity and inhibits inflammatory signaling [110, 111]. However, in obesity and other metabolic disorders, adipose tissue undergoes structural and functional remodeling [112, 113]. This includes adipocyte hypertrophy, extracellular matrix expansion, and infiltration of pro-inflammatory immune cells, particularly macrophages [113, 114]. These changes result in a chronic, low-grade inflammatory state characterized by elevated secretion of cytokines such as TNF- $\alpha$ , IL-6, and monocyte chemoattractant protein-1 (MCP-1) [115]. The resulting inflammatory milieu disrupts insulin signaling pathways and contributes to systemic insulin resistance and metabolic dysfunction [115]. Furthermore, the bidirectional communication between adipocytes and immune cells via adipokines, chemokines, and extracellular vesicles reinforces the inflammatory state [116]. This inflammation links dysfunctional adipose tissue to conditions such as T2D, CVD, and non-alcoholic fatty liver disease [117, 118].

Emerging evidence suggests that adipose tissue is also affected by systemic iron dysregulation [119]. Under conditions of iron overload, excess iron may accumulate in both adipocytes and resident immune cells, particularly macrophages [119]. This can amplify oxidative stress through Fenton chemistry, leading to increased production of ROS and further activation of pro-inflammatory pathways [120]. Iron-induced oxidative stress has been shown to downregulate adiponectin and impair insulin

signaling in adipocytes [121]. In addition, iron accumulation in adipose-resident macrophages promotes cytokine release and contributes to local inflammation [122, 123]. Elevated iron accumulation within adipose tissue has been associated with increased inflammatory markers and metabolic disturbances in both animal models and human studies, implying that proper regulation of iron levels is essential for preserving adipose tissue integrity and function [123].

### **1.8 Adiponectin**

As described in section 1.7, adiponectin is a protein hormone predominantly secreted by mature adipocytes and is classified as a member of the adipokine family. Unlike many pro-inflammatory adipokines, adiponectin stands out for its beneficial effects on metabolic homeostasis, particularly in enhancing insulin sensitivity. It circulates in relatively high concentrations in the bloodstream and exerts systemic effects on various target tissues, including the liver, skeletal muscle, and vascular endothelium [125]. Functionally, adiponectin activates key metabolic pathways, including AMP-activated protein kinase (AMPK) and peroxisome proliferator-activated receptor alpha (PPAR- $\alpha$ ), which are central to metabolic regulation and cellular stress responses. Adiponectin also modulates immune cell function, particularly by regulating cytokine expression and maintaining immune balance.

Due to its beneficial metabolic and anti-inflammatory functions, adiponectin has attracted considerable interest in clinical research. Decreased level of circulating adiponectin are consistently associated with obesity, type 2 diabetes, cardiovascular disease, and non-alcoholic fatty liver disease [129-131]. As a result, strategies aimed at increasing adiponectin levels or mimicking its activity have been explored as potential therapeutic interventions. For example, in preclinical models, artificially synthetic adiponectin receptor agonists and adiponectin-mimetic peptides have shown ability to improve insulin sensitivity, reducing hepatic lipid accumulation, and attenuating inflammation [132, 133]. Moreover, certain pharmacological agents—such as thiazolidinediones—may exert part of their therapeutic effect by upregulating adiponectin expression [134, 135]. Although clinical translation remains in early stages, targeting the adiponectin pathway continues to be a compelling approach in the treatment of metabolic and inflammatory disorders.

### **1.9 ALY688**

Although adiponectin has shown considerable therapeutic potential due to its anti-inflammatory and insulin-sensitizing functions, its direct clinical application faces significant challenges. As a full-length protein hormone with 244 amino acids, human adiponectin is difficult to synthesize and deliver efficiently in vivo due to its complex multimeric structure, short half-

life, and poor bioavailability [125]. Moreover, recombinant adiponectin requires high production costs and poses challenges related to stability and tissue targeting [136]. These limitations have prompted the development of alternative compounds that can activate adiponectin signaling pathways while possessing improved pharmacological properties. ALY688 is an adiponectin receptor agonist with only 13 amino acids [137]. This short synthetic peptide is derived from the globular domain of adiponectin, exhibiting enhanced stability, favorable bioavailability, and the ability to selectively bind and activate AdipoR1 and AdipoR2, thereby reproducing many of the downstream metabolic and anti-inflammatory effects of native adiponectin [138, 139].

The development of ALY688 was based on a structure-guided approach aiming to identify peptides that could replicate the bioactivity of adiponectin. Scientists began by screening a library of peptide fragments derived from the globular domain of adiponectin, focusing on sequences that retained receptor-binding capacity and functional activity [140]. Through iterative screening and optimization, a specific short peptide sequence—later named ALY688—was identified for its strong affinity toward AdipoR1 and AdipoR2 receptors [140]. Preclinical studies confirmed that ALY688 could activate downstream signaling pathways such as AMPK and PPAR- $\alpha$ , leading to metabolic and anti-inflammatory effects similar to those of native adiponectin [140]. Figure 4 shows how ALY688 can activate

adiponectin receptor signaling, leading to downstream activation of AMPK and Nrf2 pathways. This activation results in reduced oxidative stress, suppression of pro-inflammatory transcription factors such as NF $\kappa$ B.

Several studies have employed ALY688 to investigate its potential therapeutic roles in metabolic and inflammatory conditions. In models of insulin resistance and obesity, ALY688 administration improved glucose tolerance and reduced hepatic lipid accumulation [138-141]. In cardiovascular research, ALY688 has been shown to protect against myocardial ischemia-reperfusion injury by modulating inflammation and oxidative stress pathways [142]. Additionally, recent studies have explored its effects in the models of muscular dystrophy, liver fibrosis, and neuroinflammation, highlighting its broad therapeutic applicability [138, 143, 144]. These findings suggest that ALY688 may serve as a versatile tool for studying adiponectin signaling and as a candidate for future clinical translation in diseases characterized by metabolic dysfunction and chronic inflammation.

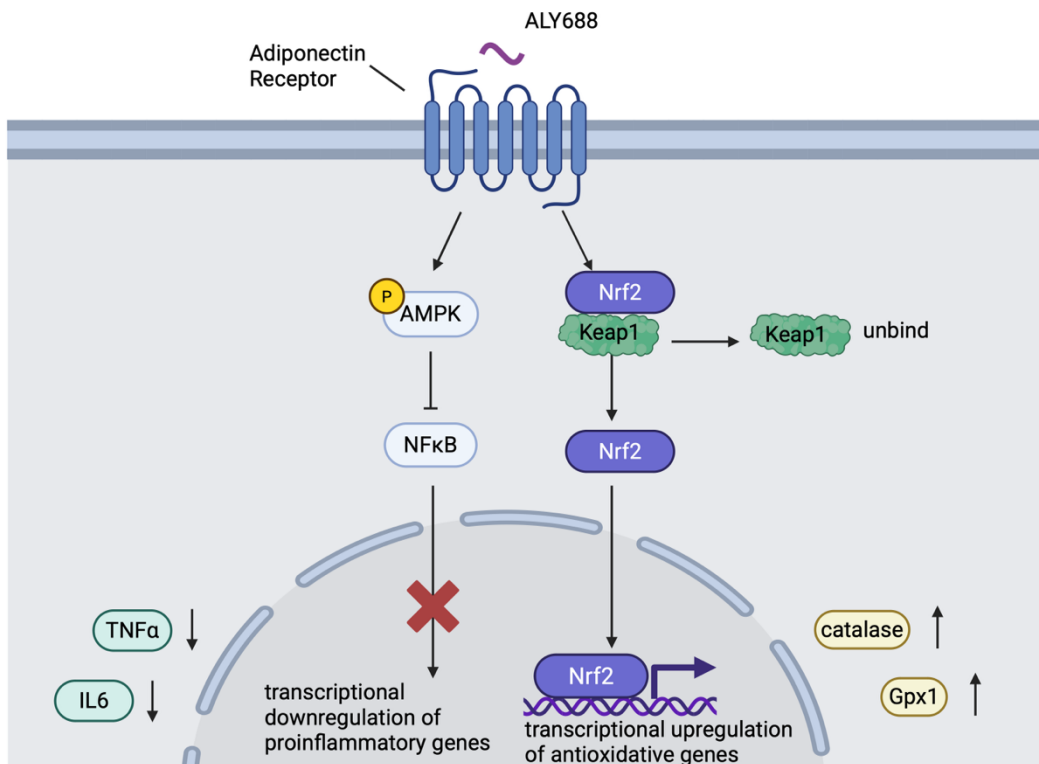


**Figure 4. ALY688-mediated activation of adiponectin receptor signaling attenuates inflammation via AMPK and Nrf2 pathways.** Upon activation by ALY688, AdipoR activates downstream pathways such as AMPK and Nrf2, which can inhibit inflammatory transcription factors and suppress oxidative stress. This modulation attenuates NFκB-mediated expression of pro-inflammatory cytokines such as IL6 and TNFα. Once ALY688 stimulates AdipoR, Nrf2 is released from binding of Keap1-mediated sequestration in the cytoplasm. Activated Nrf2 then translocates into the nucleus, leading to the upregulation of antioxidant and detoxifying gene, for example, GPX1 and catalase, thereby reducing intracellular ROS levels and limiting oxidative damage.

## **Chapter 2**

**“ALY688 attenuates iron overload-induced inflammation  
in RAW 264.7 macrophages by reducing oxidative stress”**

## 2.1 Hypothesis

Previous studies have shown that among immune cells, macrophages are particularly sensitive to iron fluctuations due to their role in red blood cells recycling and homeostasis [94]. Excess intracellular iron can reprogram macrophages toward a pro-inflammatory state characterized by increased cytokine and redox imbalance [147]. I hypothesize that iron overload will induce an inflammatory response in RAW 264.7 macrophages, leading to the increased expression of pro-inflammatory cytokines, such as TNF and IL-1 $\beta$ , through ROS-mediated activation of NF- $\kappa$ B and IRF pathways. To test this hypothesis, I would treat RAW264.7 cells with ferrous sulfate and measure the expression of inflammatory cytokines by qPCR, as well as monitor pathway activation using luciferase reporter assays.

ALY688 has been demonstrated to bind to both AdipoR1 and AdipoR2 receptors, resulting in adiponectin-like responses in various experimental models [137]. This makes ALY688 a promising candidate for testing its impact on adiponectin signaling and its potential anti-inflammatory effects in macrophages under conditions of iron overload. Furthermore, ALY688 has the advantage of being a small molecule, which allows for easier production and application compared to recombinant adiponectin [137]. Thus, ALY688 represents a promising candidate for evaluating adiponectin signaling and its anti-inflammatory effects under iron overload conditions. I would further hypothesize that ALY688 can mitigate these iron-induced

inflammatory responses by modulating oxidative stress pathways and attenuating ROS accumulation, thereby reducing inflammation. As a result, ALY688 treatment may decrease pro-inflammatory cytokine production and restore inflammatory homeostasis in macrophages. To test this hypothesis, ALY688 would be administered as a pretreatment to assess its protective effects on iron-induced inflammation and ROS production.

## **2.2 Study aims and significance**

### **Study aims**

1. To determine the optimal iron concentration and time course for triggering an inflammatory response in RAW 264.7 macrophages.
2. To investigate the anti-inflammatory potential of ALY688.
3. To explore the mechanism by which ALY688 attenuates inflammatory responses.

### **Significance of the study**

This study provides new insights into how iron overload induces inflammation in macrophages through oxidative stress pathways. It also highlights the therapeutic potential of ALY688 in mitigating iron-induced inflammatory responses, suggesting a novel approach for managing chronic inflammation.

## 2.3 Experimental models

For this study, I used RAW264.7 cells, a murine macrophage-like cell line. This cell line is widely used for mechanistic studies of macrophage activation and polarization due to its responsiveness to inflammatory stimuli and ease of genetic and pharmacological manipulation [151]. Compared to primary macrophages, RAW264.7 cells offer several advantages, including ease of use and safety, as well as faster growth rates compared to primary cells [151]. Additionally, the homogeneous genetic background of the RAW264.7 cell line reduces variability in macrophage phenotypes, providing more consistent and reproducible results in experiments [151]. These features make RAW264.7 cells an ideal model for investigating macrophage functions, especially in the context of inflammation and immune response modulation.

To further elucidate the signaling pathways involved in iron-induced inflammation, this study utilized DUAL-RAW reporter cells—an engineered derivative of the RAW 264.7 macrophage line. These cells are stably transfected with two different reporter systems: one that expresses Lucia luciferase driven by an interferon regulatory factor (IRF)-responsive promoter, and another that expresses secreted embryonic alkaline phosphatase (SEAP) regulated by an NF- $\kappa$ B-responsive promoter. By using the dual-reporter system, the activation of NF- $\kappa$ B and IRF pathway activation in response to pro-inflammatory stimuli can be monitored

simultaneously and quantitatively. NF- $\kappa$ B is a key transcription factor in mediating the expression of pro-inflammatory cytokines such as IL-6 and TNF- $\alpha$ , and is activated by stimuli including toll-like receptors (TLRs), tumor necrosis factor receptors (TNFRs), and interleukin-1 receptors (IL-1Rs). The IRF pathway, particularly IRF3 and IRF7, plays a central role in antiviral responses and type I interferon production but also contributes to inflammation in macrophages under stress conditions such as iron overload. By using this dual-reporter system, we aimed to dissect the dynamic involvement of these two canonical inflammatory pathways in iron-induced macrophage activation and evaluate how ALY688 modulates their activity.

## **2.4 Methods**

### **Cell culture and treatment**

RAW 264.7 (ATCC® TIB-71TM) mouse macrophages were cultured in Gibco® high glucose (+4.5g/L D-glucose, +L-glutamine, -sodium pyruvate, cat # 11965084) Dulbecco's Modified Eagle's Medium (DMEM) supplemented with 10% heat-inactivated fetal bovine serum (FBS) and 1% (v/v) penicillin streptomycin at 37°C with 95% air and 5% CO<sub>2</sub>. Cells were maintained in T75 (growth area per well: 75 cm<sup>2</sup>) flasks and passed at 70% confluency. Cell scrapers were used to detach the cells from the flasks. Cells were then seeded in a density of 1X 10<sup>4</sup> cells per well.

For iron overload treatment, iron (II) sulfate heptahydrate ( $\text{FeSO}_4 \cdot 7\text{H}_2\text{O}$ ) (Sigma-Aldrich; #215422) was prepared by dissolving in sterile distilled water with the stock concentration of 100mM, which was aliquoted and stored at  $-4^\circ\text{C}$ . Prior to use, the stock was diluted in serum free high glucose DMEM to a final concentration of 100 $\mu\text{M}$ . Cells were then treated for 1, 2, 4, or 6 hours.

For ALY688 pretreatment, a 1mM stock solution was prepared in serum free high glucose DMEM to a final concentration of 100nM ALY688 (Allysta Pharmaceuticals), and cells were treated for 30 minutes or 16 hours. After ALY688 pretreatment, the cells received iron overload treatment. I used ALY688 pretreatment to evaluate its potential preventive role in mitigating iron-induced inflammation, rather than assessing its therapeutic effects after cellular damage had already occurred. This approach also can minimize the possibility that iron overload might interfere with ALY688 uptake or its intracellular signaling efficacy.

### **RAW-Dual™ (IRF-Lucia/KI-[MIP-2] SEAP) reporter cells and luciferase assays**

Activation of NF- $\kappa\text{B}$  and IRF signaling pathways was assessed by using RAW-Dual™ (InvioGen, IRF-Lucia/KI-[MIP-2] SEAP, cat. # rawd-ismip) reporter cells and luciferase assays. LPS treatment was used as a positive control. Untreated cells were included as the negative control. Cells were

seeded into flat-bottom 96-well plates at a density of  $1 \times 10^5$  cells/well in DMEM with 10% FBS. After overnight incubation, cells were treated with varying concentrations of ferrous sulfate ( $\text{FeSO}_4$ ) (25, 50, 100, 150, 200  $\mu\text{M}$ ) for different time periods (1, 3, 6, or 12 hours). In experiments involving anti-inflammatory pretreatment, cells were pretreated with 100 nM ALY688 (Allysta Pharmaceuticals), stock: 1 mM in sterile water, stored at  $-20^\circ\text{C}$ ) for either 30 minutes or 16 hours before iron exposure. LPS treatment (100ng/ml) was used as a positive control. Untreated cells were included as a negative control. For IRF pathway activity detection, 20  $\mu\text{l}$  of culture supernatant was transferred to a white opaque 96-well plate, and 50  $\mu\text{l}$  of QUANTI-Luc™ 4 reagent (InvivoGen, cat. # rep-qlc-4lg1) was added. Luminescence was immediately measured using a luminometer, and results were expressed as relative light units (RLU). For NF- $\kappa\text{B}$  activity, 20  $\mu\text{l}$  of supernatant was mixed with 180  $\mu\text{l}$  of QUANTI-Blue™ Solution in a separate 96-well plate, subsequently incubated at  $37^\circ\text{C}$  for 5 hours, and optical density (OD) was measured at 620-655 nm using a microplate reader.

### **Time-course measurement of intracellular iron using colorimetric ferrozine-based assay**

Intracellular iron levels were quantified using a modified ferrozine-based colorimetric assay. RAW 264.7 macrophages were seeded in a 24-

well plate and incubated at 37°C overnight. Once the cells reached 70% confluency, they were treated with 100µM ferrous sulfate for 1, 2, 4, or 6 hours in serum-free HG DMEM. Following treatment, cells were washed three times with cold PBS to remove extracellular iron.

To release intracellular iron, 200µl of 50mM NaOH, 200µl of 10mM HCl, and 200µl of freshly prepared iron-releasing agent (IRA; a 1:1 mixture of 1.4 M HCl and 4.5% KMnO<sub>4</sub>) were sequentially added to each well. Plates were sealed with aluminum foil and incubated at 60 °C for 2 hours.

After incubation, 60 µl of iron detection reagent (IDR) was added to each well. The IDR consisted of 6.5 mM ferrozine, 6.5 mM neocuproine, 2.5 M ammonium acetate, and 1.0 M ascorbic acid. Plates were incubated at room temperature for 30 minutes to allow colour development.

Subsequently, 280 µl of the reaction mixture from each well was transferred into a 96-well plate, and absorbance was measured at 550 nm using a microplate reader. Standard curves were generated using FeSO<sub>4</sub> standard solutions (0–300 µM in 10 mM HCl) to calculate absolute intracellular iron concentrations.

### **Detecting intracellular iron using FerroOrange reagent**

Intracellular ferrous iron (Fe<sup>2+</sup>) levels were visualized using FerroOrange (Dojindo; #F374), a selective fluorescent probe for labile Fe<sup>2+</sup>. RAW 264.7 macrophages were seeded in an 8-well chamber slide and

incubated overnight at 37 °C in a 5% CO<sub>2</sub> atmosphere. After reaching appropriate confluency, cells were treated with or without 100 μM ferrous sulfate (FeSO<sub>4</sub>) for 6 hours to induce iron overload.

Following treatment, cells were washed three times with serum-free DMEM to remove background signal from serum components. A working solution of FerroOrange (1 μM) was freshly prepared by diluting a 1 mM DMSO stock solution 1:1000 in serum-free DMEM. The probe-containing medium (200 μl per well) was added to the cells, and incubation was performed at 37 °C for 30 minutes in the dark.

Without further washing, cells were immediately imaged using a confocal fluorescence microscope (excitation: 561 nm; emission: 570–620 nm). Fluorescence intensity was quantified using ImageJ by selecting regions of interest (ROIs) corresponding to individual cells.

Quantified fluorescence values were exported to GraphPad Prism for statistical analysis. Comparisons were made between the control group and the 6-hour iron-treated group using unpaired two-tailed Student's t-test. Results were expressed as mean ± standard error of the mean (SEM), and  $p < 0.05$  was considered statistically significant.

### **Gene expression analysis**

RAW 264.7 macrophages were seeded in 6-well plates and cultured until reaching approximately 70% confluency. Cells were then treated with

FeSO<sub>4</sub> (100 μM) for 6 hours in high glucose DMEM with 0% FBS. At the end of the treatment, cells were washed three times with ice-cold PBS and lysed for total RNA extraction using the RNeasy Mini Kit (QIAGEN). The RNA concentration and purity were measured using the μDrop™ Plate and a plate reader (Thermo Fisher, Waltham, MA, USA). Approximately 400 ng of total RNA per sample was reverse transcribed into complementary DNA (cDNA) using the RevertAid RT Reverse Transcription Kit (Thermo Fisher) with random hexamer primers. qPCR reactions were prepared with cDNA, iQ™ SYBR® Green Supermix (Bio-Rad, Hercules, CA, USA), and gene-specific primers. Amplification was carried out on a Bio-Rad real-time PCR machine using the following cycling conditions: initial enzyme activation at 95 °C, followed by cycles of denaturation at 95 °C, annealing at 60 °C, and extension at 72 °C. A plate read was conducted after each cycle. Relative gene expression was calculated using the 2<sup>^(-ΔΔCt)</sup> method, normalized to β-actin rRNA. Primers used in this study are summarized in Table 1.

Name	Kind	Sequences (5'-3')
TNF	Forward	CAGGCGGTGCCTATGTCTC
	Reverse	CGATCACCCCGAAGTTCAGTAG
IL6	Forward	CTGCAAGAGACTTCCATCCAG
	Reverse	AGTGGTATAGACAGGTCTGTTGG
IL-1β	Forward	GAAATGCCACCTTTTGACAGTG

	Reverse	TGGATGCTCTCATCAGGACAG
IL-10	Forward	CTTACTGACTGGCATGAGGATCA
	Reverse	GCAGCTCTAGGAGCATGTGG
IFNb	Forward	GCCTTTGCCATCCAAGAGATGC
	Reverse	ACACTGTCTGCTGGTGGAGTTC
IFNa	Forward	TGCCCAGCAGATCAAGAAGG
	Reverse	TCAGGGGAAATTCCTGCACC
NOX2	Forward	AGTGCGTGTTGCTCGACAA
	Reverse	GCGGTGTGCAGTGCTATCAT
SOD1	Forward	AACCAGTTGTGTTGTCAGGAC
	Reverse	CCACCATGTTTCTTAGAGTGAGG
SOD2	Forward	CAGACCTGCCTTACGACTATGG
	Reverse	CTCGGTGGCGTTGAGATTGTT
Gpx1	Forward	CCACCGTGTATGCCTTCTCC
	Reverse	AGAGAGACGCGACATTCTCAAT
Catalase	Forward	GGAGGCGGGAACCCAATAG
	Reverse	GTGTGCCATCTCGTCAGTGAA

**Table 1. List of Primers used**

### **Detecting oxidative stress using CellROXTM Deep Red reagent**

Reactive oxygen species (ROS) levels were evaluated using CellROX®

Deep Red fluorescent probes. CellROX Deep Red is non-fluorescent in its

reduced form and emits strong fluorescence upon oxidation. For live-cell ROS detection, RAW 264.7 macrophages were seeded at approximately 70% confluency in high glucose DMEM with 0% FBS on 96 well plates. Prior to imaging, cells were stained with Hoechst 33342 (100 nM) and CellROX® Deep Red (2.5  $\mu$ M) simultaneously for 30 minutes in high glucose DMEM without FBS. The images were acquired using the EVOS fluorescence microscope, enabling visualization and comparison of ROS accumulation across different treatment groups with a 20 $\times$  objective in a 37 °C, 5% CO<sub>2</sub> live-cell imaging chamber. Hydrogen peroxide (H<sub>2</sub>O<sub>2</sub>, 100 $\mu$ M) was used as a positive control to induce oxidative stress and validate the CellROX staining system. N-acetylcysteine (NAC, 500 nM) served as an antioxidant reference.

### **Statistical analysis**

Statistical analysis was conducted by using GraphPad Prism 9. Differences between groups were evaluated using either t-tests or a one-way ANOVA. All experiments were performed with a minimum of three biological replicates (n = 3). Data are expressed as mean  $\pm$  SEM, and a p-value of less than 0.05 was considered statistically significant.

## 2.5 Results

### 1. Iron treatment induces inflammatory responses and elevates intracellular iron levels in a time dependent manner.

To investigate whether iron overload induces inflammatory signaling in macrophages, RAW-Dual<sup>TM</sup> receptor cells were treated with increasing concentrations of ferrous sulfate ( $\text{FeSO}_4$ , 50–200  $\mu\text{M}$ ) for 1, 3, 6, and 12 hours. Lucia luciferase activity, which reflects IRF pathway activation, showed a mild increase at one hour (Figure 5A), followed by significant elevation at 3, 6, and 12 hours of treatment, particularly at higher concentrations (100–200  $\mu\text{M}$ ) (Figure 5B, 5C, and 5D). Notably, the response further increased at 12 hours, reaching the highest levels observed (Figure D), indicating a progressive and sustained activation of the IRF signaling pathway. LPS treatment (100ng/ml) served as a positive control and elicited robust luciferase activity in each time course.

In parallel, NF- $\kappa$ B pathway activation was evaluated by quantifying SEAP expression. A mild increase was observed at one hour (Figure 5E), most evident at 150  $\mu\text{M}$  and 200 $\mu\text{M}$   $\text{FeSO}_4$ . After six hours of treatment, SEAP levels were significantly elevated at 100 $\mu\text{M}$   $\text{FeSO}_4$ , suggesting that NF- $\kappa$ B signaling is responsive to iron overload in a time-dependent manner.

To determine whether iron overload leads to intracellular iron accumulation, RAW 264.7 macrophages were treated with 100  $\mu\text{M}$   $\text{FeSO}_4$  for six hours and subsequently stained with FerroOrange. Confocal

microscopy revealed markedly increased fluorescence in iron-treated cells compared to control (Figure 5G), and quantitative analysis confirmed a significant elevation in intracellular Fe<sup>2+</sup> levels (Figure 1H, \*\*\*\*p<0.0001). In addition, a ferrozine-based colorimetric assay demonstrated a time-dependent increase in intracellular iron content from one to six hours (Figure 5I), further supporting enhanced iron uptake under iron overload conditions.

Together, these findings demonstrate that ferrous iron overload activates IRF and NF- $\kappa$ B inflammatory signaling pathways in a time and concentration dependent manner, with a robust response detectable at six hours with 100  $\mu$ M FeSO<sub>4</sub>. Concurrently, intracellular iron accumulation increases over time, confirming effective iron uptake in RAW 264.7 macrophages.

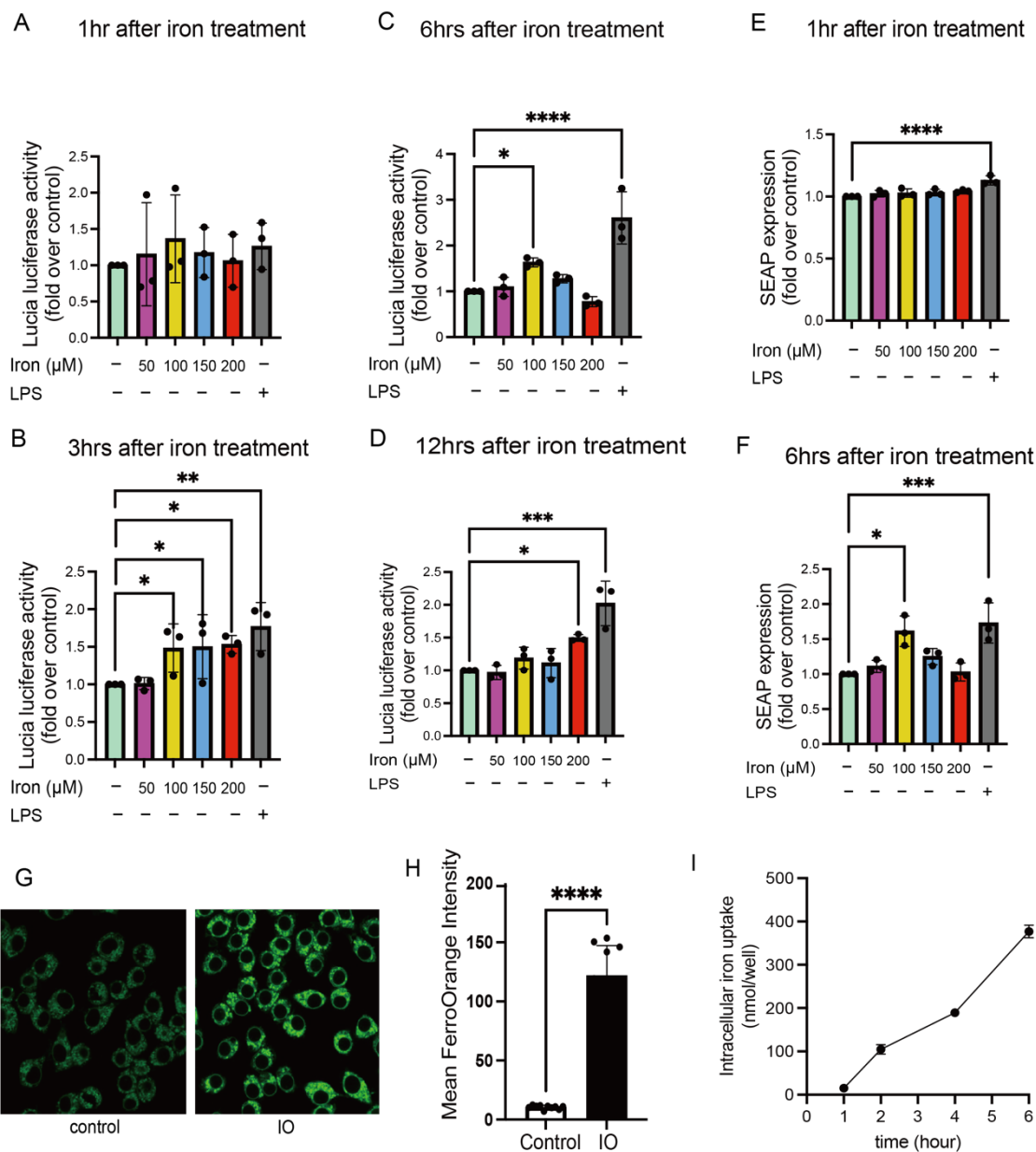


**Figure 5. Time and concentration dependent effects of Iron overload on inflammatory signaling and iron uptake in RAW 264.7 macrophages. (A–D).** IRF pathway activation was assessed by measuring Lucia luciferase activity in the supernatant of RAW-Dual™ cells treated with ferrous sulfate ( $\text{FeSO}_4$ , 50–200  $\mu\text{M}$ ) for 1 hr (A, n=3), 3 hrs (B, n=3), 6 hrs (C, n=3), and 12 hrs (D, n=3), or with LPS (100ng/mL) as a positive control. **(E–F).** NF- $\kappa$ B pathway activation was evaluated by quantifying SEAP expression at 1 hr (E, n=3) and 6 hrs (F, n=3) after iron treatment. **(G–I).** Iron uptake was assessed using multiple complementary approaches. (G)

Representative confocal images of intracellular Fe<sup>2+</sup> levels using FerroOrange staining after 6 hrs iron treatment (100 μM FeSO<sub>4</sub>). (H) Quantification of FerroOrange fluorescence intensity shows significantly increased intracellular Fe<sup>2+</sup> in the iron-treated group compared to control (n=10). (I) Time-dependent intracellular iron accumulation was measured using a ferrozine-based colorimetric assay following 1, 2, 4, and 6 h of 100 μM FeSO<sub>4</sub> treatment (n=3 per time point). All quantitative data are presented as mean ± SEM. Statistical significance was determined by unpaired Student's t-test or one-way ANOVA with appropriate post hoc tests. \*p < 0.05, \*\*p < 0.01, \*\*\*\*p < 0.0001.

## **2. ALY688 attenuates iron-induced proinflammatory gene expression in DUAL-RAW cells.**

To examine whether ALY688 can mitigate the inflammatory effects of iron overload, RAW-Dual™ reporter cells were treated with 100 μM FeSO<sub>4</sub> (iron overload, IO) for 6 hours with or without pretreatment with ALY688 (100 nM, 16 hours). Lucia luciferase activity, indicating IRF pathway activation, was markedly increased by IO treatment and strongly suppressed by ALY688 (Figure 6A). This suggests that ALY688 can effectively inhibit type I interferon-related inflammatory signaling induced by iron overload.

NF-κB activity, as measured by SEAP expression, was similarly elevated by IO and significantly reduced by ALY688 pretreatment (Figure 6B). The strongest SEAP induction was observed in the IO and LPS groups, while ALY688 pretreatment (100nM, 16 hours) substantially attenuated the NF-κB response. This indicates that ALY688 is capable of interfering with canonical NF-κB signaling, potentially through inhibition of upstream

kinases such as IKK $\beta$  or through AMPK activation, which is known to negatively regulate NF- $\kappa$ B transcriptional activity. These results demonstrate that ALY688 suppresses both key inflammatory signaling pathways activated under iron overload conditions, underscoring its broad anti-inflammatory potential.

To further confirm the anti-inflammatory effects of ALY688, qPCR was performed to quantify mRNA expression of inflammatory cytokines after 16-hour ALY688 treatment (Figure 6C-H). Significant downregulation of IL6, IL1B, TNF, and IFN $\beta$  mRNA was observed (Figure 6C, 6E, 6F, 6H), consistent with inhibition of both NF- $\kappa$ B and IRF signaling pathways at the transcriptional level, suggesting that ALY688 has anti-inflammatory effects even in the absence of acute inflammatory stimuli like iron. Notably, IL10 expression was moderately increased, suggesting that ALY688 may also promote an anti-inflammatory shift in macrophage phenotype. Given that IL10 suppresses both NF- $\kappa$ B and IRF signaling via STAT3 activation, this upregulation may further contribute to a feedback inhibition loop. No significant change was observed in IFN $\alpha$  (Figure 6G), indicating that ALY688 selectively suppresses specific responses rather than a global suppression.

Together, these findings demonstrate that ALY688 pretreatment suppresses iron-induced activation of both IRF and NF- $\kappa$ B pathways and

reshapes the macrophage inflammatory profile, reducing pro-inflammatory gene expression while enhancing anti-inflammatory signaling.

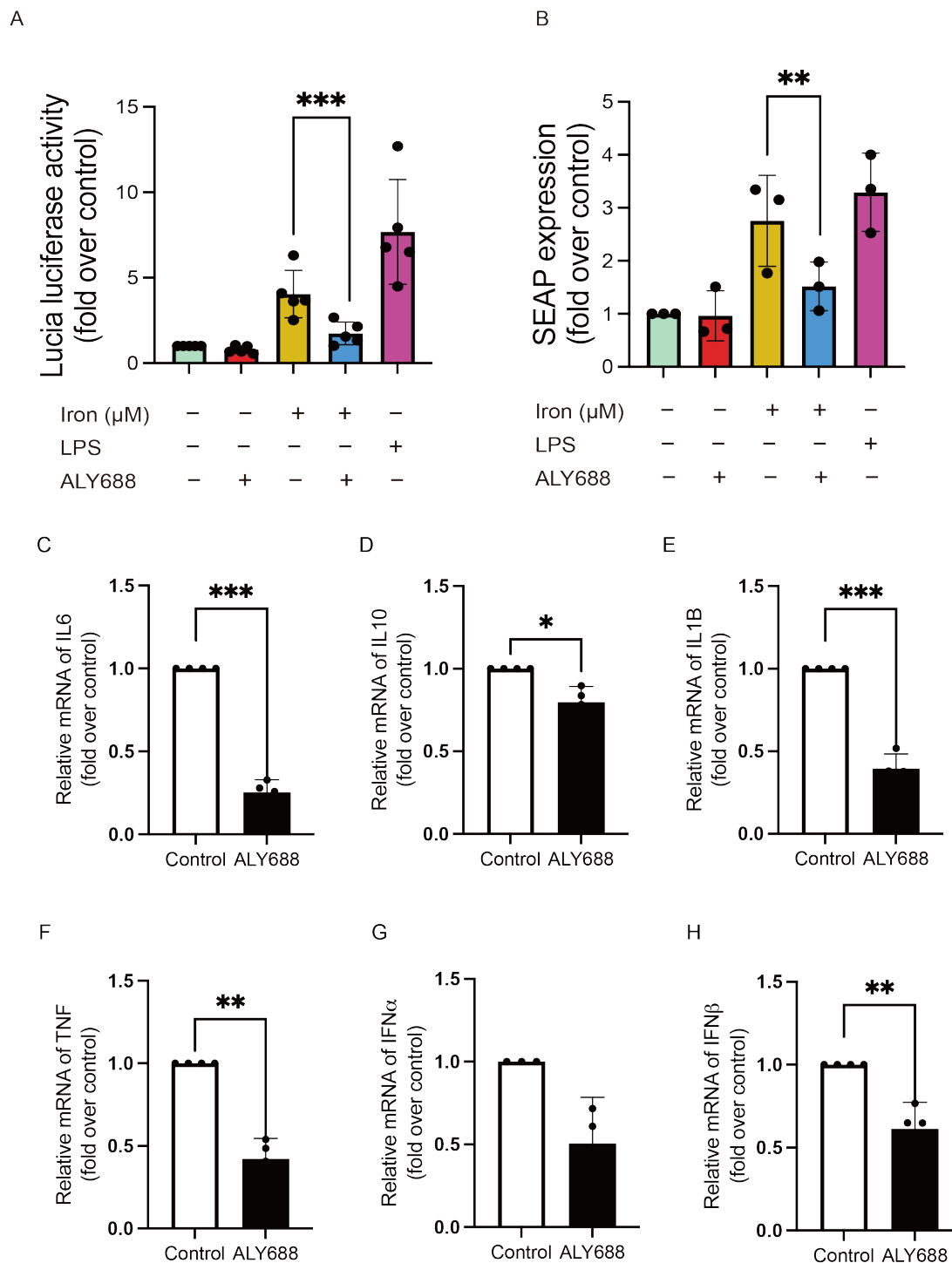


**Figure 6. ALY688 reduces inflammatory responses induced by iron overload in RAW 264.7 macrophages.** **A.** IRF pathway activation was evaluated by measuring Lucia luciferase activity after 6-hour treatment with 100  $\mu\text{M}$   $\text{FeSO}_4$  (iron overload, IO), with or without 16 hours 100 nM ALY688 pretreatment.  $n=5$ . \*\*\* $p < 0.001$  compared to IO. **B.** NF- $\kappa\text{B}$  pathway activation was assessed via SEAP expression. ALY688 alone had no effect, but pretreatment markedly reduced IO-induced SEAP levels.  $n=3$ . \*\* $p < 0.01$  compared to IO. **C-H.** real-time qPCR analysis of proinflammatory and anti-inflammatory genes. RAW 264.7 macrophages were treated with or without

100 nM ALY688 for 16 hours. ALY688 significantly downregulated IL6 (**C**), IL1B (**E**), TNF (**F**), and IFN $\beta$  (**H**), while slightly upregulated IL10 (**D**). No significant change was observed in IFN $\alpha$  (**G**). n=4 for C-F and H; n=3 for G. All gene expression values were normalized to reference genes and shown as fold change relative to control. Data are shown as mean  $\pm$  SEM. Statistical significance was determined by one-way ANOVA with appropriate post hoc tests (A-B) or unpaired two-tailed Student's t-test (C-H) \*p < 0.05, \*\*p < 0.01, \*\*\*p < 0.001, \*\*\*\*p < 0.0001.

### 3. **ALY688 reduces iron overload-induced oxidative stress and modulates antioxidant gene expression in macrophages.**

To investigate the mechanism by which ALY688 reduces iron overload-induced inflammation, we assessed whether its effects involve modulation of oxidative stress. RAW 264.7 macrophages were stained with CellROX® Deep Red to detect intracellular ROS levels after 1, 2, 4, and 6 hours of iron treatment (100  $\mu$ M FeSO<sub>4</sub>), with or without ALY688 pretreatment. As shown in the representative fluorescence images (Figure 7A-D), iron overload induced a marked increase in ROS levels over time, whereas pretreatment with ALY688 (100nM, 16 hours) visibly reduced ROS accumulation at two, four, and six hours.

Quantification of mean CellROX fluorescence intensity confirmed a time-dependent increase in ROS in iron-treated cells, which was significantly attenuated by ALY688 pretreatment (Figure 7E). These results indicate that ALY688 effectively alleviates iron-induced oxidative stress in macrophages.

To further explore the underlying mechanisms, the expression of oxidative stress-related genes was assessed by qPCR following the 16-hour ALY688 treatment. ALY688 significantly downregulated NOX2 expression (Figure 7F), a major ROS-producing enzyme, suggesting that the reduced ROS levels may be partially due to suppressed NOX2 transcription. In addition, ALY688 significantly increased the expression of Gpx1 (Figure 7G) and catalase (Figure 7J), two key antioxidant enzymes, indicating a potential enhancement of the cellular antioxidant defense system. Expression of SOD1 and SOD2 (Figure 7H and 7I) showed no significant difference between ALY688 pretreated group and control, suggesting that the antioxidant effects of ALY688 may be gene specific.

Together, these findings demonstrate that ALY688 alleviates iron-induced oxidative stress by reducing ROS accumulation and modulating the expression of both pro-oxidant and antioxidant genes in RAW 264.7 macrophages.

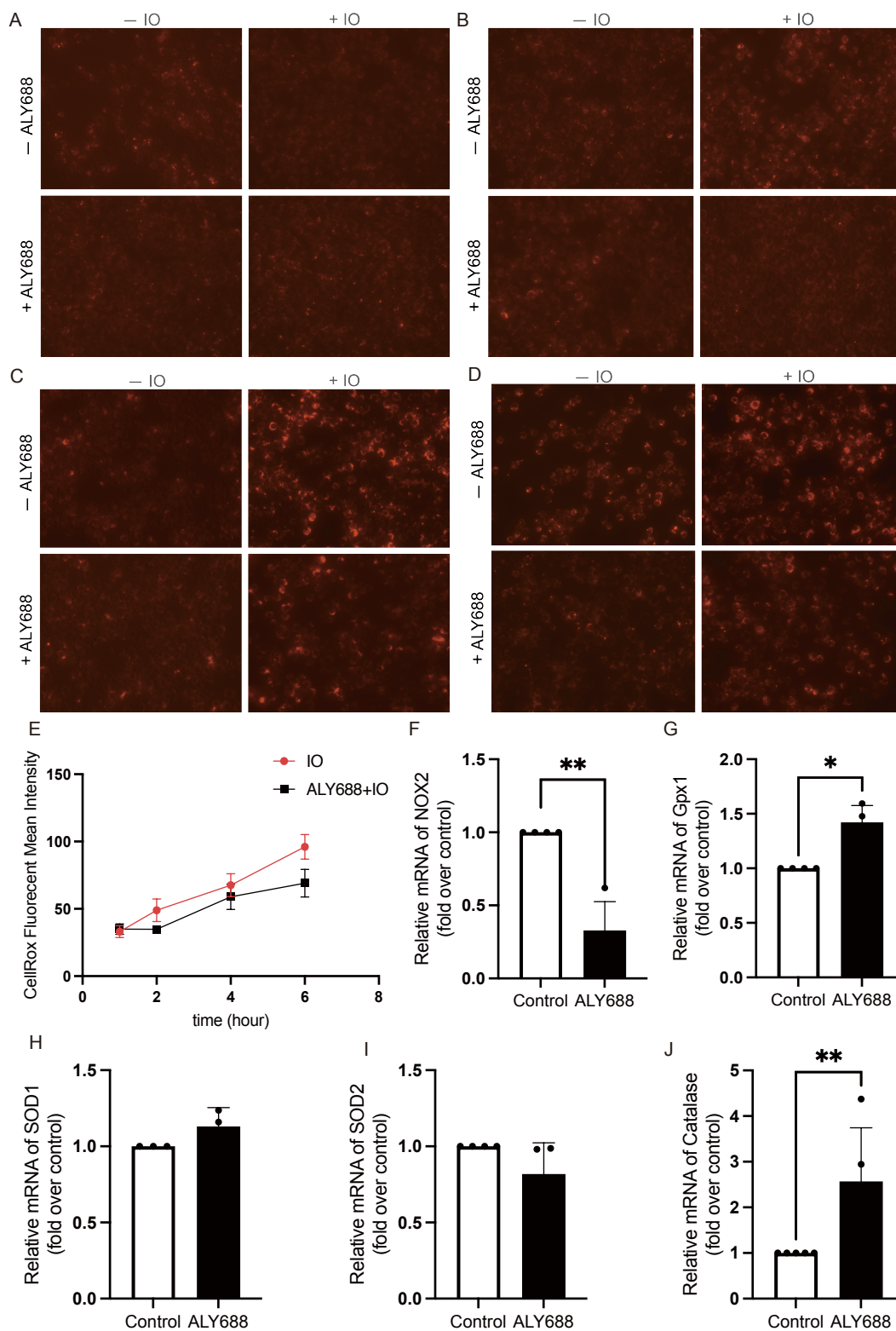


**Figure 7. ALY688 attenuates iron-induced oxidative stress and regulates expression of oxidative stress-related genes in RAW 264.7 macrophages. A–D. Representative images of CellROX® Deep Red staining in RAW 264.7**

macrophages under indicated conditions. Cells were treated with or without ALY688 (100 nM, 30 min) followed by iron overload (100  $\mu$ M FeSO<sub>4</sub>) for 1, 2, 4, or 6 hours. CellROX staining reveals increased ROS accumulation in iron-treated cells, which was visibly reduced in the ALY688+IO group across time points. **E.** Quantification of CellROX mean fluorescence intensity over time in IO versus ALY688+IO groups shows that ALY688 significantly attenuated iron-induced ROS accumulation.

**F–J.** qPCR analysis of oxidative stress-related genes. ALY688 treatment (100 nM, 16 hours) significantly decreased NOX2 expression (F), while increasing Gpx1 (G) and catalase (J) expression. No significant changes were observed in SOD1 (H) and SOD2 (I) expression. Data are presented as mean  $\pm$  SEM. Statistical significance was assessed by unpaired Student's t-test or two-way ANOVA. \* $p < 0.05$ , \*\* $p < 0.01$ .

## 2.6 Discussion

Chronic low-grade inflammation is increasingly recognized as a common pathophysiological mechanism underlying a wide spectrum of metabolic and psychiatric disorders [152]. T2D, CVD, and NAFLD are all linked to persistent inflammatory signaling, with macrophage activation playing a key role in disease progression [153]. T2D affected an estimated 8.8% of the global population in 2015, and this figure is projected to reach 10.4% by 2040 [154]. Importantly, emerging evidence suggests that low-grade inflammation is also implicated in neuropsychiatric conditions such as anxiety disorders, highlighting the systemic impact of immune dysregulation [155]. Among the various triggers of chronic inflammation, iron overload has gained increased attention because of its ability to promote oxidative stress and inflammatory responses in macrophages. Despite this, therapeutic strategies that directly address iron-induced inflammation remain limited. In this study, we investigated whether ALY688,

a synthetic agonist of adiponectin receptors, could attenuate iron-induced macrophage activation and explored its underlying anti-inflammatory mechanisms.

Our results demonstrate that iron overload activates both the IRF and NF- $\kappa$ B signaling pathways in RAW 264.7 macrophages, as indicated by luciferase and SEAP expression dual reporter assays. This activation was associated with increased expression of multiple pro-inflammatory genes, including IL-6, TNF, IL-1 $\beta$ , IFN- $\alpha$ , and IFN- $\beta$ , as measured by qPCR. In addition, iron treatment significantly elevated intracellular ROS levels, as shown by CellROX staining, indicating a state of oxidative stress. Pretreatment with ALY688 markedly suppressed both inflammatory signaling and ROS accumulation. Furthermore, ALY688 increased the expression of key antioxidant genes such as catalase and Gpx1, suggesting that its protective effects may involve the restoration of redox homeostasis. Together, these results indicate that ALY688 reduces iron-induced macrophage inflammation by inhibiting ROS production and downregulating pro-inflammatory pathways.

Iron overload has long been associated with tissue injury and immune dysfunction. The pro-inflammatory effects of iron overload on macrophages have been extensively studied. Prior studies have shown that iron accumulation promotes the pro-inflammatory polarization of macrophages, enhances cytokine production, and induces oxidative stress via ROS-

dependent mechanisms [156]. For example, in 2019, Hu and colleagues demonstrated that excess iron shifts macrophage metabolism towards glycolysis, a metabolic profile that supports M1 polarization and enhances inflammatory responses [153]. This metabolic reprogramming contributes not only to macrophage activation but also to the progression of atherosclerosis. Moreover, Zhou et al. reported that iron overload upregulates ROS production by promoting p53 acetylation and increasing the activity of P300/CBP acetyltransferases, further driving M1-type differentiation [68]. These findings collectively underscore the central role of macrophages in mediating iron-induced inflammation. Consistent with these reports, our study demonstrated that iron overload activates pro-inflammatory signaling pathways in macrophages, upregulating key cytokines such as IL-6, TNF, IL-1 $\beta$ , IFN- $\alpha$ , and IFN- $\beta$ , while also significantly increasing intracellular ROS levels. These results confirm that RAW264.7 macrophages respond to excess iron with robust inflammatory and oxidative stress responses, supporting the existing mechanistic understanding of iron-induced immune activation. Importantly, our findings also reveal that ALY688 effectively counteracts these responses. To our knowledge, this is the first study to demonstrate the potential of ALY688 in suppressing iron-induced macrophage activation. Our lab has previously shown that ALY688 confers protective effects against liver injury, enhances insulin sensitivity, and exhibits anti-inflammatory properties in models of

cardiac dysfunctions [142]. These current findings expand the therapeutic potential of ALY688 to inflammation driven by iron overload, and highlight its relevance in targeting macrophage-mediated immune activation.

My results showed that ALY688 can effectively inhibit type I interferon-related inflammatory signaling induced by iron overload, supporting the link between iron overload and chronic inflammation, as type I interferons are known mediators of chronic inflammatory responses. This suppression of type I interferon-related inflammatory signaling may involve modulation of the IRF3/7 axis or upstream TLR-TRIF signaling pathways. Importantly, the lack of effect by ALY688 alone supports its role as a conditional modulator, requiring an inflammatory trigger to exert its action. The underlying mechanism by which iron promotes inflammation appears to center around ROS generation and redox imbalance. Iron catalyzes the generation of hydroxyl radicals via the Fenton reaction, which in turn cause oxidative damage and activation of downstream pathways such as NF- $\kappa$ B and IRF [40]. My CellROX data confirm that iron-treated macrophages exhibit significant ROS accumulation, and the reduction of ROS by ALY688 strongly correlates with suppression of inflammatory signaling. Moreover, ALY688 upregulates antioxidant enzymes, indicating it may enhance the cell's intrinsic defense systems. This is consistent with previous studies suggesting that adiponectin activates AMPK signaling, which are known to modulate oxidative stress and inflammation [157]. My findings suggest that

ALY688 mitigates iron-induced inflammation via a mechanism involving both reduced ROS production and enhanced antioxidant gene expression. Interestingly, although ALY688 significantly upregulated the expression of Gpx1 and catalase, which are key enzymes involved in hydrogen peroxide detoxification, it did not induce significant changes in SOD1 or SOD2, which primarily remove superoxide radicals. Given that catalase and GPx1 act downstream to convert hydrogen peroxide into water and oxygen, this observation may suggest that ALY688 preferentially enhances the removal of hydrogen peroxide downstream of ROS generation, rather than inhibiting superoxide formation at the initial stage. Supporting this, CellROX fluorescence intensity was significantly reduced in cells treated with hydrogen peroxide plus ALY688 pretreatment, compared to cells treated with hydrogen peroxide alone, suggesting that ALY688 may facilitate hydrogen peroxide detoxification (data not shown). Further investigation is needed to elucidate whether this selective upregulation reflects differential transcriptional regulation or post-transcriptional stability of antioxidant enzymes.

These findings highlight the potential of ALY688 as a therapeutic candidate for diseases characterized by iron overload and macrophage-driven inflammation. Conditions such as hereditary hemochromatosis, transfusion-dependent anemias, and chronic liver diseases often feature elevated tissue iron and persistent immune activation; yet effective anti-

inflammatory interventions are lacking. By targeting both oxidative stress and inflammatory signaling, ALY688 may offer a dual-action strategy to reduce tissue damage and promote immune resolution. Although our study was limited to in vitro experiments, it lays the foundation for future in vivo investigations to evaluate the systemic efficacy and safety of ALY688 in relevant disease models.

## **2.7 Conclusion**

In summary, the data presented in this study indicate that ALY688 exerts a modulatory effect on iron overload-induced oxidative stress and inflammatory responses in RAW 264.7 macrophages. Treatment with ALY688 led to a reduction in pro-inflammatory gene expression and attenuated activation of the IRF signaling pathway, supporting its potential anti-inflammatory properties. Furthermore, ALY688 partially reversed iron-induced oxidative stress, as evidenced by changes in antioxidant gene expression and decreased intracellular ROS levels, particularly under iron overload conditions. Collectively, these findings highlight ALY688 as a promising candidate for alleviating iron-induced inflammation and oxidative damage. However, further studies with increased biological replicates and mechanistic investigations are warranted to validate these effects and elucidate the pathways involved.

### **CHAPTER 3**

### **CONCLUSIONS**

### 3.1 Thesis Summary

Iron overload is increasingly recognized as a contributor to chronic low-grade inflammation, particularly through its effects on macrophage activation. Macrophages exposed to excess iron tend to polarize toward the pro-inflammatory M1 phenotype, generating reactive oxygen species (ROS) and producing elevated levels of inflammatory cytokines. However, strategies to mitigate iron-induced macrophage inflammation remain limited.

In this study, I investigated the anti-inflammatory potential of ALY688, a synthetic Adiponectin receptor agonist, in a model of iron overload-induced macrophage activation using RAW 264.7 cells. Our data demonstrated that iron overload activated both NF- $\kappa$ B and IRF pathways, increased intracellular ROS, and upregulated pro-inflammatory cytokines, including IL-1 $\beta$ , IL-6, TNF- $\alpha$ , IFN- $\alpha$ , and IFN- $\beta$ . Treatment with ALY688 significantly suppressed these inflammatory responses. Notably, ALY688 enhanced the expression of antioxidant enzymes Gpx1 and catalase, which are key players in hydrogen peroxide detoxification, suggesting that its anti-inflammatory effect may be partly mediated through ROS modulation. Interestingly, no significant changes were observed in SOD1 or SOD2, indicating that ALY688 may preferentially act downstream in the oxidative stress pathway. Overall, our findings identify ALY688 as a potential therapeutic agent for alleviating iron-induced inflammation and provide mechanistic insights into how targeting AdipoR

signaling may modulate macrophage activation under oxidative stress conditions.

### **3.2 Study Limitations**

Several limitations should be acknowledged in this study. First, all experiments were conducted in vitro using the RAW 264.7 murine macrophage cell line. While this model is widely used to study macrophage responses, it does not fully capture the complexity of macrophage behavior in vivo, especially within the context of tissue-specific microenvironments or systemic iron metabolism. RAW 246.7 macrophages may differ in responsiveness, receptor expression, and metabolic state compared to tissue-resident macrophages in organs, such as adipose tissue and liver. Therefore, the findings may not fully reflect macrophage behaviour under systemic iron overload conditions in an organismal context. Second, although ALY688 treatment significantly attenuated inflammatory gene expression and ROS levels, the precise signaling mechanisms downstream of AdipoR activation—such as AMPK or PPAR pathways—were not directly examined in this study. Previous literature has implicated AMPK activation, ceramidase activity, and PPA $\alpha$  signaling in mediating AdipoR [111]. Third, while we observed selective upregulation of Gpx1 and catalase, functional assays to quantify actual enzymatic activity or ROS breakdown rates were not performed, limiting the interpretation of how ALY688 accelerates the antioxidant response. Enzyme activity assays or redox-

sensitive biosensors could provide a more functional view of antioxidant capacity. Additionally, the study focused primarily on transcriptional and fluorescence-based analyses; future work incorporating protein-level validation (e.g., Western blotting) and in vivo models will be critical to further substantiate the therapeutic potential of ALY688 under conditions of iron overload. Finally, the study employed a specific set of iron concentrations and treatment time points. Although they were sufficient to induce inflammation and ROS production, they may not capture the full dose-response dynamics or longer-term effects of chronic iron exposure. A more comprehensive time-course and dose-response analysis would strengthen conclusions about the threshold and kinetics of iron-induced inflammation and ALY688's modulatory effects.

### **3.3 Future Works**

Based on the current findings, several works for future research are proposed to improve our understanding of ALY688's anti-inflammatory potential and its underlying mechanisms. First, to extend the relevance of our in vitro findings, future studies should evaluate the effects of ALY688 in animal models of systemic or tissue-specific iron overload, such as dietary iron-loading mice. Assessing inflammatory cytokine levels, macrophage polarization, and tissue ROS burden in vivo would provide critical evidence for ALY688's translational potential. Second, further investigation into the upstream signaling pathways involved in ALY688-mediated antioxidant

gene regulation (such as Nrf2 activation) would clarify how ALY688 selectively modulates ROS-scavenging systems like GPx1 and catalase, while having limited effects on SOD1 and SOD2. Third, expanding the analysis to other immune cell types, such as dendritic cells or monocytes, may reveal whether the effects of ALY688 are macrophage-specific or part of a broader immunomodulatory mechanism. Finally, given the emerging literature on extracellular vesicles, future work could explore whether EVs derived from iron-overloaded macrophages carry pro-inflammatory or iron-regulatory signals, and whether ALY688 alters the contents or functions of these EVs. Notably, recent findings demonstrated that macrophage-derived EVs can act as endogenous iron chelators and protect against iron overload-induced cardiac injury in a myocardial infarction model, highlighting their potential as therapeutic vectors [158]. Inspired by this, further studies may evaluate whether ALY688 modulates the cargo composition or iron-buffering capacity of macrophage-derived EVs, thus offering a novel cell-free strategy to mitigate iron-associated inflammation and tissue damage.

## References

1. Vogt, A.S., et al., *On Iron Metabolism and Its Regulation*. Int J Mol Sci, 2021. **22**(9).
  2. Muckenthaler, M.U., B. Galy, and M.W. Hentze, *Systemic iron homeostasis and the iron-responsive element/iron-regulatory protein (IRE/IRP) regulatory network*. Annu Rev Nutr, 2008. **28**: p. 197-213.
  3. Roemhild, K., et al., *Iron metabolism: pathophysiology and pharmacology*. Trends Pharmacol Sci, 2021. **42**(8): p. 640-656.
  4. Ems, T., K. St Lucia, and M.R. Huecker, *Biochemistry, Iron Absorption*, in *StatPearls*. 2025, StatPearls Publishing
- Copyright © 2025, StatPearls Publishing LLC.: Treasure Island (FL).
5. Papanikolaou, G. and K. Pantopoulos, *Iron metabolism and toxicity*. Toxicol Appl Pharmacol, 2005. **202**(2): p. 199-211.
  6. Dixon, S.J. and B.R. Stockwell, *The role of iron and reactive oxygen species in cell death*. Nat Chem Biol, 2014. **10**(1): p. 9-17.
  7. Wang, J. and K. Pantopoulos, *Regulation of cellular iron metabolism*. Biochem J, 2011. **434**(3): p. 365-81.
  8. Kakhlon, O. and Z.I. Cabantchik, *The labile iron pool: characterization, measurement, and participation in cellular processes(1)*. Free Radic Biol Med, 2002. **33**(8): p. 1037-46.
  9. Konijn, A.M., et al., *The cellular labile iron pool and intracellular ferritin in K562 cells*. Blood, 1999. **94**(6): p. 2128-34.

10. Gordan, R., et al., *Involvement of cytosolic and mitochondrial iron in iron overload cardiomyopathy: an update*. Heart Fail Rev, 2018. **23**(5): p. 801-816.
11. Zhang, D.L., et al., *A ferroportin transcript that lacks an iron-responsive element enables duodenal and erythroid precursor cells to evade translational repression*. Cell Metab, 2009. **9**(5): p. 461-73.
12. Charlebois, E., et al., *A crosstalk between hepcidin and IRE/IRP pathways controls ferroportin expression and determines serum iron levels in mice*. Elife, 2022. **11**.
13. Theil, E.C., *Ferritin: the protein nanocage and iron biomineral in health and in disease*. Inorg Chem, 2013. **52**(21): p. 12223-33.
14. Li, L., et al., *Binding and uptake of H-ferritin are mediated by human transferrin receptor-1*. Proc Natl Acad Sci U S A, 2010. **107**(8): p. 3505-10.
15. Fillebeen, C., et al., *Transferrin receptor 1 controls systemic iron homeostasis by fine-tuning hepcidin expression to hepatocellular iron load*. Blood, 2019. **133**(4): p. 344-355.
16. Shieh, J.T., et al., *Heterozygous Nonsense Variants in the Ferritin Heavy Chain Gene FTH1 Cause a Novel Pediatric Neuroferritinopathy*. medRxiv, 2023.
17. Anderson, G.J. and D.M. Frazer, *Current understanding of iron homeostasis*. Am J Clin Nutr, 2017. **106**(Suppl 6): p. 1559S-1566S.

18. Lakhal-Littleton, S., et al., *Cardiac ferroportin regulates cellular iron homeostasis and is important for cardiac function*. Proc Natl Acad Sci U S A, 2015. **112**(10): p. 3164-9.
19. Kowdley, K.V., et al., *Hepcidin Signaling in Health and Disease: Ironing Out the Details*. Hepatol Commun, 2021. **5**(5): p. 723-735.
20. <Tam\_Eddie\_2023\_Masters.pdf>.
21. Ebner, N. and S. von Haehling, *Iron deficiency in heart failure: a practical guide*. Nutrients, 2013. **5**(9): p. 3730-9.
22. Comín-Colet, J., et al., *Iron deficiency is a key determinant of health-related quality of life in patients with chronic heart failure regardless of anaemia status*. Eur J Heart Fail, 2013. **15**(10): p. 1164-72.
23. Punnonen, K., K. Irjala, and A. Rajamäki, *Serum transferrin receptor and its ratio to serum ferritin in the diagnosis of iron deficiency*. Blood, 1997. **89**(3): p. 1052-7.
24. Murphy, C.J. and G.Y. Oudit, *Iron-overload cardiomyopathy: pathophysiology, diagnosis, and treatment*. J Card Fail, 2010. **16**(11): p. 888-900.
25. Gattermann, N., et al., *The Evaluation of Iron Deficiency and Iron Overload*. Dtsch Arztebl Int, 2021. **118**(49): p. 847-856.
26. Kratz, A., et al., *Case records of the Massachusetts General Hospital. Weekly clinicopathological exercises. Laboratory reference values*. N Engl J Med, 2004. **351**(15): p. 1548-63.

27. Ritchie, R.F., et al., *Reference distributions for serum iron and transferrin saturation: a practical, simple, and clinically relevant approach in a large cohort*. J Clin Lab Anal, 2002. **16**(5): p. 237-45.
28. Baranwal, A.K. and S.C. Singhi, *Acute iron poisoning: management guidelines*. Indian Pediatr, 2003. **40**(6): p. 534-40.
29. Urru, S.A., et al., *Reproducibility of liver iron concentration measured on a biopsy sample: a validation study in vivo*. Am J Hematol, 2015. **90**(2): p. 87-90.
30. He, T., et al., *Myocardial T2\* measurements in iron-overloaded thalassemia: An in vivo study to investigate optimal methods of quantification*. Magn Reson Med, 2008. **60**(5): p. 1082-9.
31. Reeder, S.B., et al., *Quantification of Liver Iron Overload with MRI: Review and Guidelines from the ESGAR and SAR*. Radiology, 2023. **307**(1): p. e221856.
32. Ras-Jiménez, M.D.M., et al., *Soluble Transferrin Receptor as Iron Deficiency Biomarker: Impact on Exercise Capacity in Heart Failure Patients*. J Pers Med, 2023. **13**(8).
33. Sacri, A.-S., et al., *Hepcidin, Soluble Transferrin Receptor, and Other Biomarkers of Iron Status Distributions in Healthy 2 Years Old Infants from a National Ambulatory Study in France*. Blood, 2019. **134**(Supplement\_1): p. 4809-4809.

34. Yun, S. and N.D. Vincelette, *Update on iron metabolism and molecular perspective of common genetic and acquired disorder, hemochromatosis*. Crit Rev Oncol Hematol, 2015. **95**(1): p. 12-25.
35. Szczerbinska, A., et al., *Hemochromatosis-How Not to Overlook and Properly Manage "Iron People"-A Review*. J Clin Med, 2024. **13**(13).
36. Bacon, B.R., et al., *Diagnosis and management of hemochromatosis: 2011 practice guideline by the American Association for the Study of Liver Diseases*. Hepatology, 2011. **54**(1): p. 328-43.
37. Bardou-Jacquet, E., et al., *GNPAT variant associated with severe iron overload in HFE hemochromatosis*. Hepatology, 2015. **62**(6): p. 1917-8.
38. Barton, J.C., J.C. Barton, and R.T. Acton, *Non-alcoholic fatty liver disease in hemochromatosis probands with iron overload and HFE p.C282Y/p.C282Y*. BMC Gastroenterol, 2023. **23**(1): p. 137.
39. Mariani, R., et al., *Iron metabolism in thalassemia and sickle cell disease*. Mediterr J Hematol Infect Dis, 2009. **1**(1): p. e2009006.
40. Zubair, A., *Therapeutic phlebotomy*. Clin Liver Dis (Hoboken), 2014. **4**(5): p. 102-106.
41. Mobarra, N., et al., *A Review on Iron Chelators in Treatment of Iron Overload Syndromes*. Int J Hematol Oncol Stem Cell Res, 2016. **10**(4): p. 239-247.

42. Jakubczyk, K., et al., *Reactive oxygen species - sources, functions, oxidative damage*. Pol Merkur Lekarski, 2020. **48**(284): p. 124-127.
43. He, L., et al., *Antioxidants Maintain Cellular Redox Homeostasis by Elimination of Reactive Oxygen Species*. Cell Physiol Biochem, 2017. **44**(2): p. 532-553.
44. Brigelius-Flohé, R. and M. Maiorino, *Glutathione peroxidases*. Biochim Biophys Acta, 2013. **1830**(5): p. 3289-303.
45. Amos, D.L., et al., *Catalase overexpression modulates metabolic parameters in a new 'stress-less' leptin-deficient mouse model*. Biochim Biophys Acta Mol Basis Dis, 2017. **1863**(9): p. 2293-2306.
46. Santanam, N., et al., *Overexpression of human catalase gene decreases oxidized lipid-induced cytotoxicity in vascular smooth muscle cells*. Arterioscler Thromb Vasc Biol, 1999. **19**(8): p. 1912-7.
47. Prasad, A.S., et al., *Antioxidant effect of zinc in humans*. Free Radic Biol Med, 2004. **37**(8): p. 1182-90.
48. Schieber, M. and N.S. Chandel, *ROS function in redox signaling and oxidative stress*. Curr Biol, 2014. **24**(10): p. R453-62.
49. Batty, M., M.R. Bennett, and E. Yu, *The Role of Oxidative Stress in Atherosclerosis*. Cells, 2022. **11**(23).
50. Hurre, S. and W.H. Hsu, *The etiology of oxidative stress in insulin resistance*. Biomed J, 2017. **40**(5): p. 257-262.

51. Reynolds, A., et al., *Oxidative stress and the pathogenesis of neurodegenerative disorders*. Int Rev Neurobiol, 2007. **82**: p. 297-325.
52. Reuter, S., et al., *Oxidative stress, inflammation, and cancer: how are they linked?* Free Radic Biol Med, 2010. **49**(11): p. 1603-16.
53. Berdoukas, V., T.D. Coates, and Z.I. Cabantchik, *Iron and oxidative stress in cardiomyopathy in thalassemia*. Free Radic Biol Med, 2015. **88**(Pt A): p. 3-9.
54. Zanganeh, S., et al., *Iron oxide nanoparticles inhibit tumour growth by inducing pro-inflammatory macrophage polarization in tumour tissues*. Nat Nanotechnol, 2016. **11**(11): p. 986-994.
55. Liochev, S.I. and I. Fridovich, *The Haber-Weiss cycle -- 70 years later: an alternative view*. Redox Rep, 2002. **7**(1): p. 55-7; author reply 59-60.
56. Tam, E., et al., *Importance of Autophagy in Mediating Cellular Responses to Iron Overload in Cardiomyocytes*. Rev Cardiovasc Med, 2022. **23**(5): p. 167.
57. Li, D. and M. Wu, *Pattern recognition receptors in health and diseases*. Signal Transduction and Targeted Therapy, 2021. **6**(1): p. 291.
58. McNab, F., et al., *Type I interferons in infectious disease*. Nature Reviews Immunology, 2015. **15**(2): p. 87-103.
59. Newton, K. and V.M. Dixit, *Signaling in innate immunity and inflammation*. Cold Spring Harb Perspect Biol, 2012. **4**(3).

60. Chen, L., et al., *Inflammatory responses and inflammation-associated diseases in organs*. *Oncotarget*, 2018. **9**(6): p. 7204-7218.
61. Abdulkhaleq, L.A., et al., *The crucial roles of inflammatory mediators in inflammation: A review*. *Vet World*, 2018. **11**(5): p. 627-635.
62. Schwager, S. and M. Detmar, *Inflammation and Lymphatic Function*. *Front Immunol*, 2019. **10**: p. 308.
63. Punchard, N.A., C.J. Whelan, and I. Adcock, *The Journal of Inflammation*. *J Inflamm (Lond)*, 2004. **1**(1): p. 1.
64. Tsai, D.H., et al., *Effects of short- and long-term exposures to particulate matter on inflammatory marker levels in the general population*. *Environ Sci Pollut Res Int*, 2019. **26**(19): p. 19697-19704.
65. Furman, D., et al., *Chronic inflammation in the etiology of disease across the life span*. *Nature Medicine*, 2019. **25**(12): p. 1822-1832.
66. Fujioka, S., et al., *NF-kappaB and AP-1 connection: mechanism of NF-kappaB-dependent regulation of AP-1 activity*. *Mol Cell Biol*, 2004. **24**(17): p. 7806-19.
67. Morgan, M.J. and Z.-g. Liu, *Crosstalk of reactive oxygen species and NF-kB signaling*. *Cell Research*, 2011. **21**(1): p. 103-115.
68. Zhou, Y., et al., *Iron overloaded polarizes macrophage to proinflammation phenotype through ROS/acetyl-p53 pathway*. *Cancer Med*, 2018. **7**(8): p. 4012-4022.

69. Ikeda, Y., et al., *Association between serum ferritin and circulating oxidized low-density lipoprotein levels in patients with type 2 diabetes*. *Endocr J*, 2006. **53**(5): p. 665-70.
70. Liu, T., et al., *NF- $\kappa$ B signaling in inflammation*. *Signal Transduction and Targeted Therapy*, 2017. **2**(1): p. 17023.
71. Sivamaruthi, B.S., et al., *NF- $\kappa$ B Pathway and Its Inhibitors: A Promising Frontier in the Management of Alzheimer's Disease*. *Biomedicines*, 2023. **11**(9).
72. Hayden, M.S. and S. Ghosh, *Regulation of NF- $\kappa$ B by TNF family cytokines*. *Semin Immunol*, 2014. **26**(3): p. 253-66.
73. Guo, Q., et al., *NF- $\kappa$ B in biology and targeted therapy: new insights and translational implications*. *Signal Transduction and Targeted Therapy*, 2024. **9**(1): p. 53.
74. Makarov, S.S., *NF-kappa B in rheumatoid arthritis: a pivotal regulator of inflammation, hyperplasia, and tissue destruction*. *Arthritis Res*, 2001. **3**(4): p. 200-6.
75. Xia, Y., S. Shen, and I.M. Verma, *NF- $\kappa$ B, an active player in human cancers*. *Cancer Immunol Res*, 2014. **2**(9): p. 823-30.
76. Monaco, C., et al., *Canonical pathway of nuclear factor kappa B activation selectively regulates proinflammatory and prothrombotic responses in human atherosclerosis*. *Proc Natl Acad Sci U S A*, 2004. **101**(15): p. 5634-9.

77. Wang, L., et al., *The multiple roles of interferon regulatory factor family in health and disease*. Signal Transduct Target Ther, 2024. **9**(1): p. 282.
78. Li, K., et al., *Promising Targets for Cancer Immunotherapy: TLRs, RLRs, and STING-Mediated Innate Immune Pathways*. Int J Mol Sci, 2017. **18**(2).
79. Song, R., et al., *IRF1 governs the differential interferon-stimulated gene responses in human monocytes and macrophages by regulating chromatin accessibility*. Cell Reports, 2021. **34**(12): p. 108891.
80. Negishi, H., T. Taniguchi, and H. Yanai, *The Interferon (IFN) Class of Cytokines and the IFN Regulatory Factor (IRF) Transcription Factor Family*. Cold Spring Harb Perspect Biol, 2018. **10**(11).
81. Barton, G.M. and J.C. Kagan, *A cell biological view of Toll-like receptor function: regulation through compartmentalization*. Nat Rev Immunol, 2009. **9**(8): p. 535-42.
82. Lukhele, S., G.M. Boukhaled, and D.G. Brooks, *Type I interferon signaling, regulation and gene stimulation in chronic virus infection*. Semin Immunol, 2019. **43**: p. 101277.
83. Chen, S., et al., *Macrophages in immunoregulation and therapeutics*. Signal Transduction and Targeted Therapy, 2023. **8**(1): p. 207.
84. Tang, D., et al., *PAMPs and DAMPs: signal 0s that spur autophagy and immunity*. Immunol Rev, 2012. **249**(1): p. 158-75.

85. Sheu, K.M. and A. Hoffmann, *Functional Hallmarks of Healthy Macrophage Responses: Their Regulatory Basis and Disease Relevance*. *Annu Rev Immunol*, 2022. **40**: p. 295-321.
86. Krenkel, O. and F. Tacke, *Liver macrophages in tissue homeostasis and disease*. *Nat Rev Immunol*, 2017. **17**(5): p. 306-321.
87. Wynn, T.A. and K.M. Vannella, *Macrophages in Tissue Repair, Regeneration, and Fibrosis*. *Immunity*, 2016. **44**(3): p. 450-462.
88. Holt, M., et al., *Dissecting and Visualizing the Functional Diversity of Cardiac Macrophages*. *Circ Res*, 2024. **134**(12): p. 1791-1807.
89. Patel, B., et al., *CCR2(+) Monocyte-Derived Infiltrating Macrophages Are Required for Adverse Cardiac Remodeling During Pressure Overload*. *JACC Basic Transl Sci*, 2018. **3**(2): p. 230-244.
90. Dick, S.A., et al., *Three tissue resident macrophage subsets coexist across organs with conserved origins and life cycles*. *Sci Immunol*, 2022. **7**(67): p. eabf7777.
91. Lahaye, C., et al., *Does iron overload in metabolic syndrome affect macrophage profile? A case control study*. *J Trace Elem Med Biol*, 2021. **67**: p. 126786.
92. Virág, L., et al., *Self-defense of macrophages against oxidative injury: Fighting for their own survival*. *Redox Biol*, 2019. **26**: p. 101261.

93. Choi, H.M., et al., *Differential effect of IL-1 $\beta$  and TNF $\alpha$  on the production of IL-6, IL-8 and PGE2 in fibroblast-like synoviocytes and THP-1 macrophages*. Rheumatol Int, 2010. **30**(8): p. 1025-33.
94. Recalcati, S. and G. Cairo, *Macrophages and Iron: A Special Relationship*. Biomedicines, 2021. **9**(11).
95. Alam, Z., et al., *Counter Regulation of Spic by NF- $\kappa$ B and STAT Signaling Controls Inflammation and Iron Metabolism in Macrophages*. Cell Rep, 2020. **31**(13): p. 107825.
96. Ramos, P., et al., *Macrophages support pathological erythropoiesis in polycythemia vera and  $\beta$ -thalassemia*. Nat Med, 2013. **19**(4): p. 437-45.
97. Winn, N.C., K.M. Volk, and A.H. Hasty, *Regulation of tissue iron homeostasis: the macrophage "ferrostat"*. JCI Insight, 2020. **5**(2).
98. Mosser, D.M., K. Hamidzadeh, and R. Goncalves, *Macrophages and the maintenance of homeostasis*. Cellular & Molecular Immunology, 2021. **18**(3): p. 579-587.
99. Agoro, R., et al., *Cell iron status influences macrophage polarization*. PLOS ONE, 2018. **13**(5): p. e0196921.
100. Johnson, E.E., et al., *Role of ferroportin in macrophage-mediated immunity*. Infect Immun, 2010. **78**(12): p. 5099-106.
101. Mesquita, G., et al., *H-Ferritin is essential for macrophages' capacity to store or detoxify exogenously added iron*. Sci Rep, 2020. **10**(1): p. 3061.

102. Soares, M.P. and I. Hamza, *Macrophages and Iron Metabolism*. *Immunity*, 2016. **44**(3): p. 492-504.
103. Carobbio, S., V. Pellegrinelli, and A. Vidal-Puig, *Adipose Tissue Function and Expandability as Determinants of Lipotoxicity and the Metabolic Syndrome*. *Adv Exp Med Biol*, 2017. **960**: p. 161-196.
104. Guerre-Millo, M., *Adipose tissue hormones*. *J Endocrinol Invest*, 2002. **25**(10): p. 855-61.
105. Clemente-Suárez, V.J., et al., *The Role of Adipokines in Health and Disease*. *Biomedicines*, 2023. **11**(5).
106. Verma, S.K., et al., *Differentiating brown and white adipose tissues by high-resolution diffusion NMR spectroscopy*. *J Lipid Res*, 2017. **58**(1): p. 289-298.
107. Kotzbeck, P., et al., *Brown adipose tissue whitening leads to brown adipocyte death and adipose tissue inflammation*. *J Lipid Res*, 2018. **59**(5): p. 784-794.
108. Kahn, C.R., G. Wang, and K.Y. Lee, *Altered adipose tissue and adipocyte function in the pathogenesis of metabolic syndrome*. *J Clin Invest*, 2019. **129**(10): p. 3990-4000.
109. Raja, R., et al., *Instruction of Immunometabolism by Adipose Tissue: Implications for Cancer Progression*. *Cancers (Basel)*, 2021. **13**(13).
110. Ouchi, N. and K. Walsh, *Adiponectin as an anti-inflammatory factor*. *Clin Chim Acta*, 2007. **380**(1-2): p. 24-30.

111. Fang, H. and R.L. Judd, *Adiponectin Regulation and Function*. Compr Physiol, 2018. **8**(3): p. 1031-1063.
112. Kirichenko, T.V., et al., *The Role of Adipokines in Inflammatory Mechanisms of Obesity*. Int J Mol Sci, 2022. **23**(23).
113. Fuster, J.J., et al., *Obesity-Induced Changes in Adipose Tissue Microenvironment and Their Impact on Cardiovascular Disease*. Circ Res, 2016. **118**(11): p. 1786-807.
114. Muir, L.A., et al., *Adipose tissue fibrosis, hypertrophy, and hyperplasia: Correlations with diabetes in human obesity*. Obesity (Silver Spring), 2016. **24**(3): p. 597-605.
115. Al-Mansoori, L., et al., *Role of Inflammatory Cytokines, Growth Factors and Adipokines in Adipogenesis and Insulin Resistance*. Inflammation, 2022. **45**(1): p. 31-44.
116. Coppack, S.W., *Pro-inflammatory cytokines and adipose tissue*. Proc Nutr Soc, 2001. **60**(3): p. 349-56.
117. Mavrogiannaki, A.N. and I.N. Migdalis, *Nonalcoholic Fatty liver disease, diabetes mellitus and cardiovascular disease: newer data*. Int J Endocrinol, 2013. **2013**: p. 450639.
118. Dharmalingam, M. and P.G. Yamasandhi, *Nonalcoholic Fatty Liver Disease and Type 2 Diabetes Mellitus*. Indian J Endocrinol Metab, 2018. **22**(3): p. 421-428.

119. Hubler, M.J., K.R. Peterson, and A.H. Hasty, *Iron homeostasis: a new job for macrophages in adipose tissue?* Trends Endocrinol Metab, 2015. **26**(2): p. 101-9.
120. Chang, J.S., et al., *Serum ferritin and risk of the metabolic syndrome: a population-based study.* Asia Pac J Clin Nutr, 2013. **22**(3): p. 400-7.
121. Gabrielsen, J.S., et al., *Adipocyte iron regulates adiponectin and insulin sensitivity.* J Clin Invest, 2012. **122**(10): p. 3529-40.
122. Fernández-Real, J.M., et al., *Serum ferritin as a component of the insulin resistance syndrome.* Diabetes Care, 1998. **21**(1): p. 62-8.
123. Joffin, N., et al., *Adipose tissue macrophages exert systemic metabolic control by manipulating local iron concentrations.* Nat Metab, 2022. **4**(11): p. 1474-1494.
124. Ziemke, F. and C.S. Mantzoros, *Adiponectin in insulin resistance: lessons from translational research.* Am J Clin Nutr, 2010. **91**(1): p. 258s-261s.
125. Achari, A.E. and S.K. Jain, *Adiponectin, a Therapeutic Target for Obesity, Diabetes, and Endothelial Dysfunction.* Int J Mol Sci, 2017. **18**(6).
126. Zhou, L., et al., *Adiponectin activates AMP-activated protein kinase in muscle cells via APPL1/LKB1-dependent and phospholipase C/Ca<sup>2+</sup>/Ca<sup>2+</sup>/calmodulin-dependent protein kinase kinase-dependent pathways.* J Biol Chem, 2009. **284**(33): p. 22426-22435.

127. Liu, Z., et al., *Adiponectin reduces ER stress-induced apoptosis through PPAR $\alpha$  transcriptional regulation of ATF2 in mouse adipose.* Cell Death Dis, 2016. **7**(11): p. e2487.
128. Luo, Y. and M. Liu, *Adiponectin: a versatile player of innate immunity.* J Mol Cell Biol, 2016. **8**(2): p. 120-8.
129. Peng, J., Q. Chen, and C. Wu, *The role of adiponectin in cardiovascular disease.* Cardiovascular Pathology, 2023. **64**: p. 107514.
130. Hui, X., et al., *Adiponectin and cardiovascular health: an update.* Br J Pharmacol, 2012. **165**(3): p. 574-90.
131. Ryu, J., et al., *Adiponectin Alleviates Diet-Induced Inflammation in the Liver by Suppressing MCP-1 Expression and Macrophage Infiltration.* Diabetes, 2021. **70**(6): p. 1303-1316.
132. Kim, S., et al., *Discovery of a novel potent peptide agonist to adiponectin receptor 1.* PLOS ONE, 2018. **13**(6): p. e0199256.
133. Zhao, C., et al., *AdipoRon alleviates fatty acid-induced lipid accumulation and mitochondrial dysfunction in bovine hepatocytes by promoting autophagy.* Journal of Dairy Science, 2023. **106**(8): p. 5763-5774.
134. Yu, J.G., et al., *The effect of thiazolidinediones on plasma adiponectin levels in normal, obese, and type 2 diabetic subjects.* Diabetes, 2002. **51**(10): p. 2968-74.

135. Gustafson, B., et al., *Adiponectin gene activation by thiazolidinediones requires PPAR $\gamma$ 2, but not C/EBP $\alpha$ —evidence for differential regulation of the aP2 and adiponectin genes*. Biochemical and Biophysical Research Communications, 2003. **308**(4): p. 933-939.
136. Turer, A.T. and P.E. Scherer, *Adiponectin: mechanistic insights and clinical implications*. Diabetologia, 2012. **55**(9): p. 2319-26.
137. Sung, H.K., et al., *ALY688 elicits adiponectin-mimetic signaling and improves insulin action in skeletal muscle cells*. Am J Physiol Cell Physiol, 2022. **322**(2): p. C151-c163.
138. Dubuisson, N., et al., *The Adiponectin Receptor Agonist, ALY688: A Promising Therapeutic for Fibrosis in the Dystrophic Muscle*. Cells, 2023. **12**(16).
139. Da Eira, D., et al., *Effects of the adiponectin mimetic compound ALY688 on glucose and fat metabolism in visceral and subcutaneous rat adipocytes*. Adipocyte, 2020. **9**(1): p. 550-562.
140. Huang, Z., et al., *The adiponectin-derived peptide ALY688 protects against the development of metabolic dysfunction-associated steatohepatitis*. Clin Transl Sci, 2024. **17**(6): p. e13760.
141. Cho, S., et al., *Cardioprotection by the adiponectin receptor agonist ALY688 in a preclinical mouse model of heart failure with reduced ejection fraction (HFrEF)*. Biomedicine & Pharmacotherapy, 2024. **171**: p. 116119.

142. Cho, S., et al., *Cardioprotection by the adiponectin receptor agonist ALY688 in a preclinical mouse model of heart failure with reduced ejection fraction (HFrEF)*. Biomed Pharmacother, 2024. **171**: p. 116119.
143. Bellissimo, C.A., et al., *The slow-release adiponectin analog ALY688-SR modifies early-stage disease development in the D2.mdx mouse model of Duchenne muscular dystrophy*. Am J Physiol Cell Physiol, 2024. **326**(4): p. C1011-c1026.
144. Tang, J., et al., *Potent anti-inflammatory effects of the adiponectin receptor agonist, ALY688*. Physiology, 2023. **38**(S1): p. 5733710.
145. Simcox, J.A. and D.A. McClain, *Iron and diabetes risk*. Cell Metab, 2013. **17**(3): p. 329-41.
146. Gujja, P., et al., *Iron overload cardiomyopathy: better understanding of an increasing disorder*. J Am Coll Cardiol, 2010. **56**(13): p. 1001-12.
147. Xia, Y., et al., *Ironing Out the Details: How Iron Orchestrates Macrophage Polarization*. Front Immunol, 2021. **12**: p. 669566.
148. Ouchi, N., et al., *Adiponectin, an adipocyte-derived plasma protein, inhibits endothelial NF-kappaB signaling through a cAMP-dependent pathway*. Circulation, 2000. **102**(11): p. 1296-301.
149. Huang, H., et al., *Mechanisms for the anti-inflammatory effects of adiponectin in macrophages*. J Gastroenterol Hepatol, 2008. **23 Suppl 1**: p. S50-3.

150. Jung, H.N. and C.H. Jung, *The Role of Anti-Inflammatory Adipokines in Cardiometabolic Disorders: Moving beyond Adiponectin*. Int J Mol Sci, 2021. **22**(24).
151. Li, P., et al., *Comparative Proteomic Analysis of Polarized Human THP-1 and Mouse RAW264.7 Macrophages*. Front Immunol, 2021. **12**: p. 700009.
152. Monteiro, R. and I. Azevedo, *Chronic inflammation in obesity and the metabolic syndrome*. Mediators Inflamm, 2010. **2010**.
153. Hu, X., et al., *Iron-load exacerbates the severity of atherosclerosis via inducing inflammation and enhancing the glycolysis in macrophages*. J Cell Physiol, 2019. **234**(10): p. 18792-18800.
154. Cho, N.H., et al., *IDF Diabetes Atlas: Global estimates of diabetes prevalence for 2017 and projections for 2045*. Diabetes Res Clin Pract, 2018. **138**: p. 271-281.
155. Cen, M., et al., *Associations between metabolic syndrome and anxiety, and the mediating role of inflammation: Findings from the UK Biobank*. Brain Behav Immun, 2024. **116**: p. 1-9.
156. Ma, J., et al., *The Role of Macrophage Iron Overload and Ferroptosis in Atherosclerosis*. Biomolecules, 2022. **12**(11).
157. Nguyen, T.M.D., *Adiponectin: Role in Physiology and Pathophysiology*. Int J Prev Med, 2020. **11**: p. 136.

158. Guo, D., et al., *Macrophage-derived extracellular vesicles represent a promising endogenous iron-chelating therapy for iron overload and cardiac injury in myocardial infarction*. J Nanobiotechnology, 2024. **22**(1): p. 527.